

LIST OF FIGURES

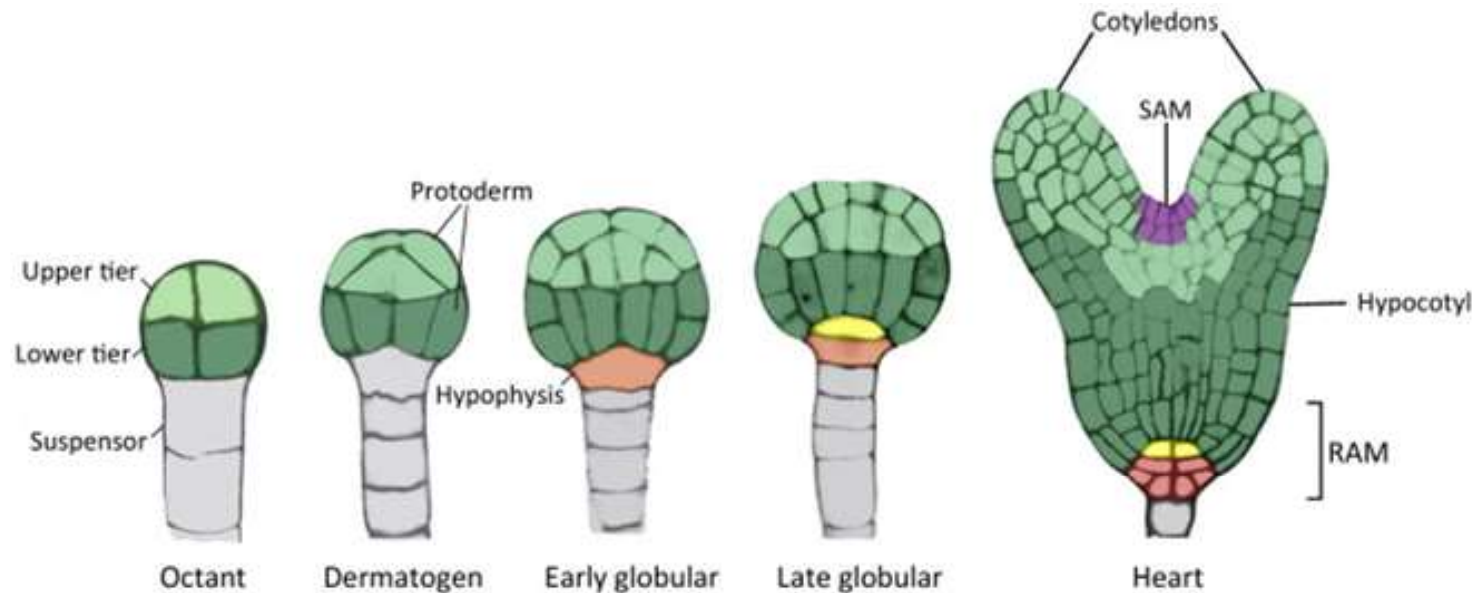


Figure 2.1 Embryo developmental stages (Zygotic embryogenesis) in *Arabidopsis*. The stages are shown here from octant to heart stages. The upper and lower tiers of the pro-embryo are established at the octant stage, which has been shown here **with light and deep green colors** respectively. Gradually, when the embryo enters to globular stage, the topmost suspensor (**here shown in grey color**) cell is described as the hypophysis (**in orange color**). Later, the hypophysis divides asymmetrically, gives rise to an apical lens-shaped cell (**in yellow color**), which act as the precursor of the QC (quiescent center) and a basal cell (in orange color), which act as the progenitor of the columella stem cells. Abbreviations: SAM, Shoot Apical Meristem; RAM, Root Apical Meristem. [Image adapted from (Radoeva and Weijers, 2014)].

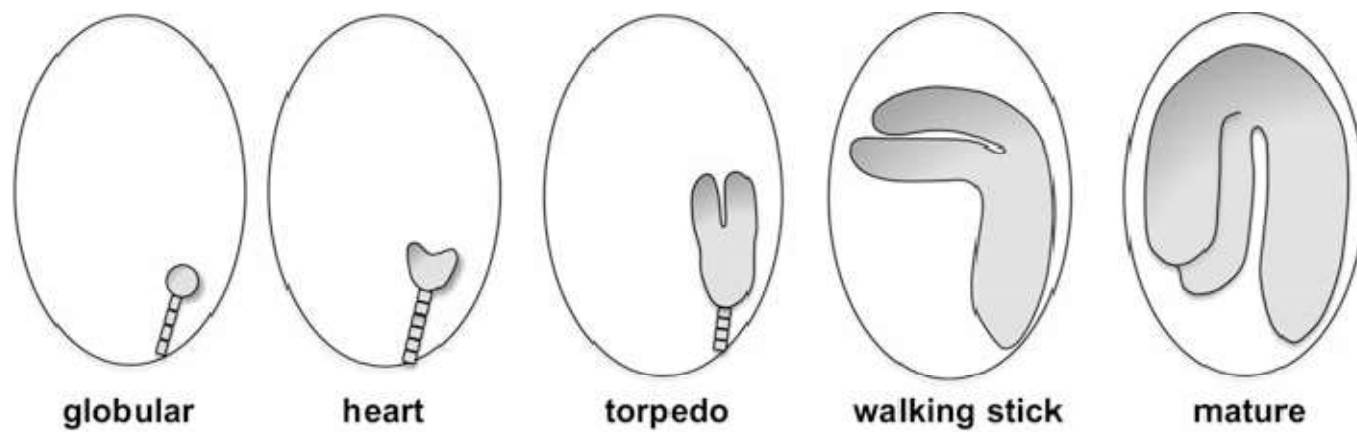


Figure 2.2. Over view of seed development stages (Adapted and modified from (Martin *et al.*, 2012))

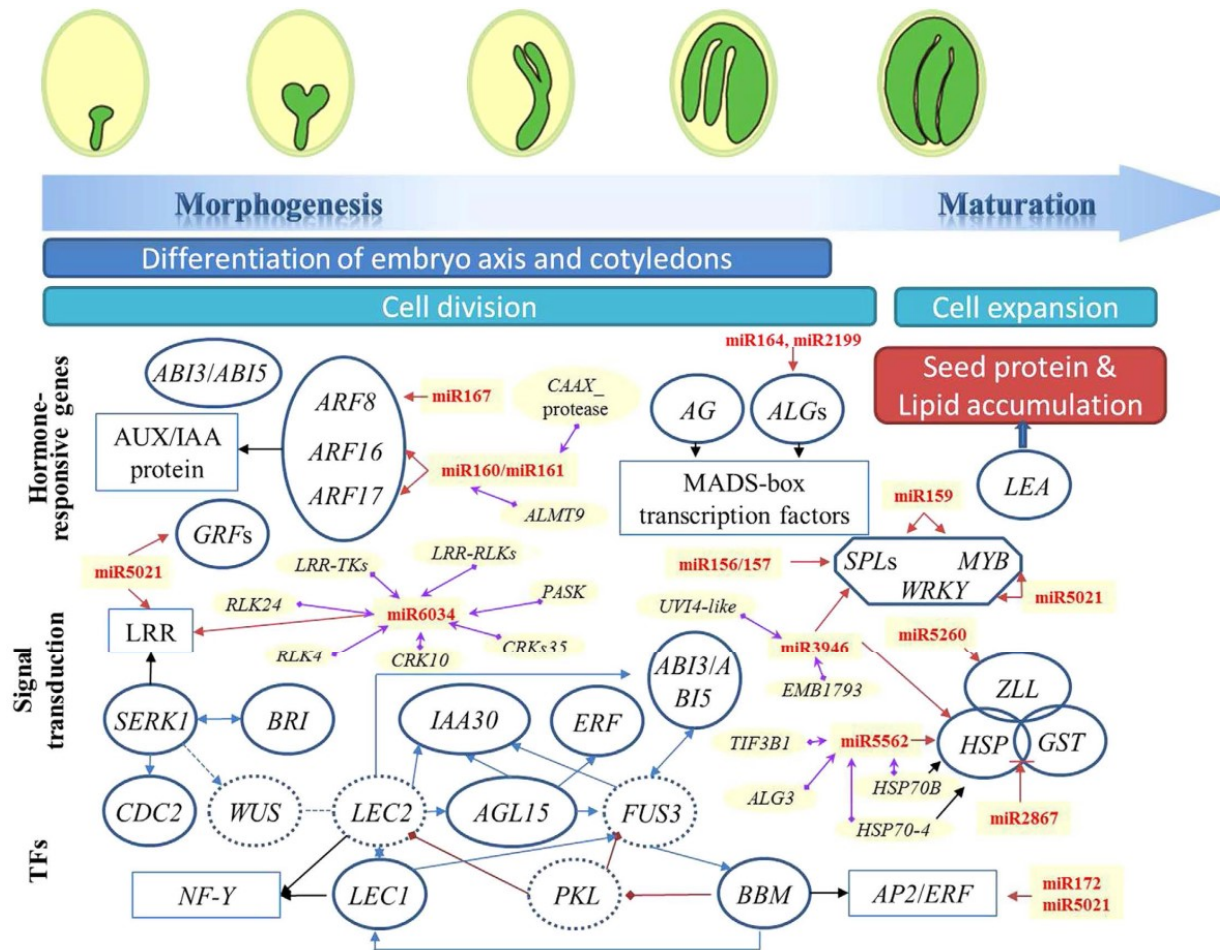


Figure 2.3 A summarised model of regulatory network depicting the genetic and molecular interactions during embryogenesis in radish. Embryo development can be categorised into two phases, morphogenesis and maturation. Arrows in blue and black colors indicate gene-like regulation and affiliation, respectively, whereas red arrows between genes indicating the transcriptional repression of the genes. The circle indicated with solid and dotted line representing those genes identified or not in radish and the corresponding miRNAs are shown in red color. Genes indicated in yellow boxes were connected with miRNAs by purple arrows which is indicating the miRNA-mRNA interactions [Image adapted from (Zhai *et al.*, 2016)].

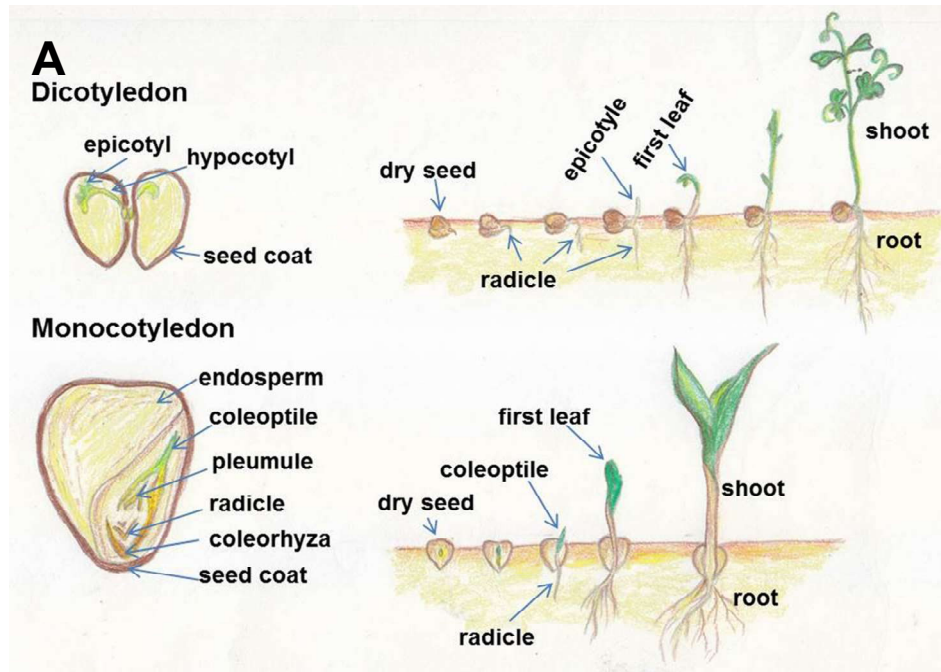


Figure 2.4A. Schematic representation of different parts of Seeds and Seed Germination stages. Seeds and germination stages of dicotyledonous (**Chickpea**) and monocotyledonous (**Maize**) plants have been shown in upper and lower panels, respectively. **B. Major Events associated with Seed Germination and Post-Germinative growth phases.** Germination stages are represented by phase 1 and phase 2; post-Germinative events includes phase 3. The time (X-Axis) for events varies from several hours to many weeks, depending on different plant species and germination conditions. Uptake of water and related increase in biomass is indicated in (Y-Axis) and shown in line graph during three phases. Some specific events (such as DNA repairing, transcription, translation and mitochondria production etc.) are spread over more than one phases and indicated with shaded color; where dark colors indicate more activity and light colors indicate less activity.

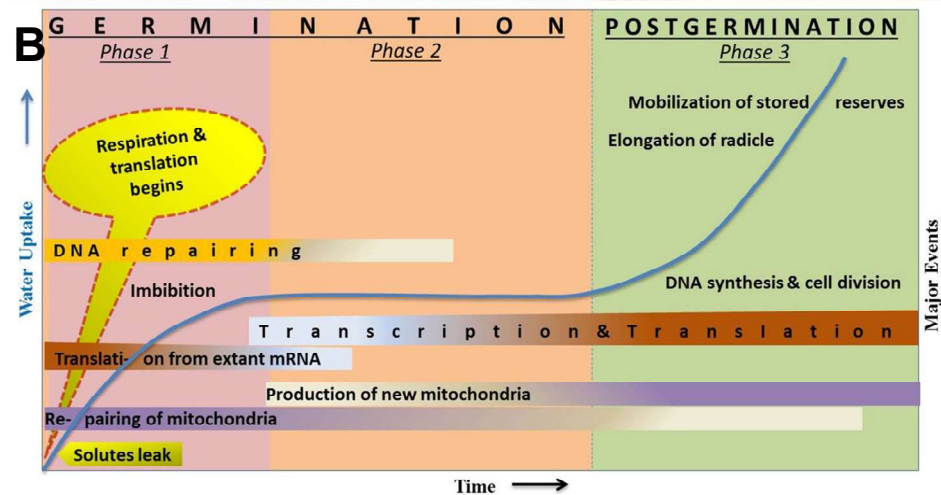


Figure 2

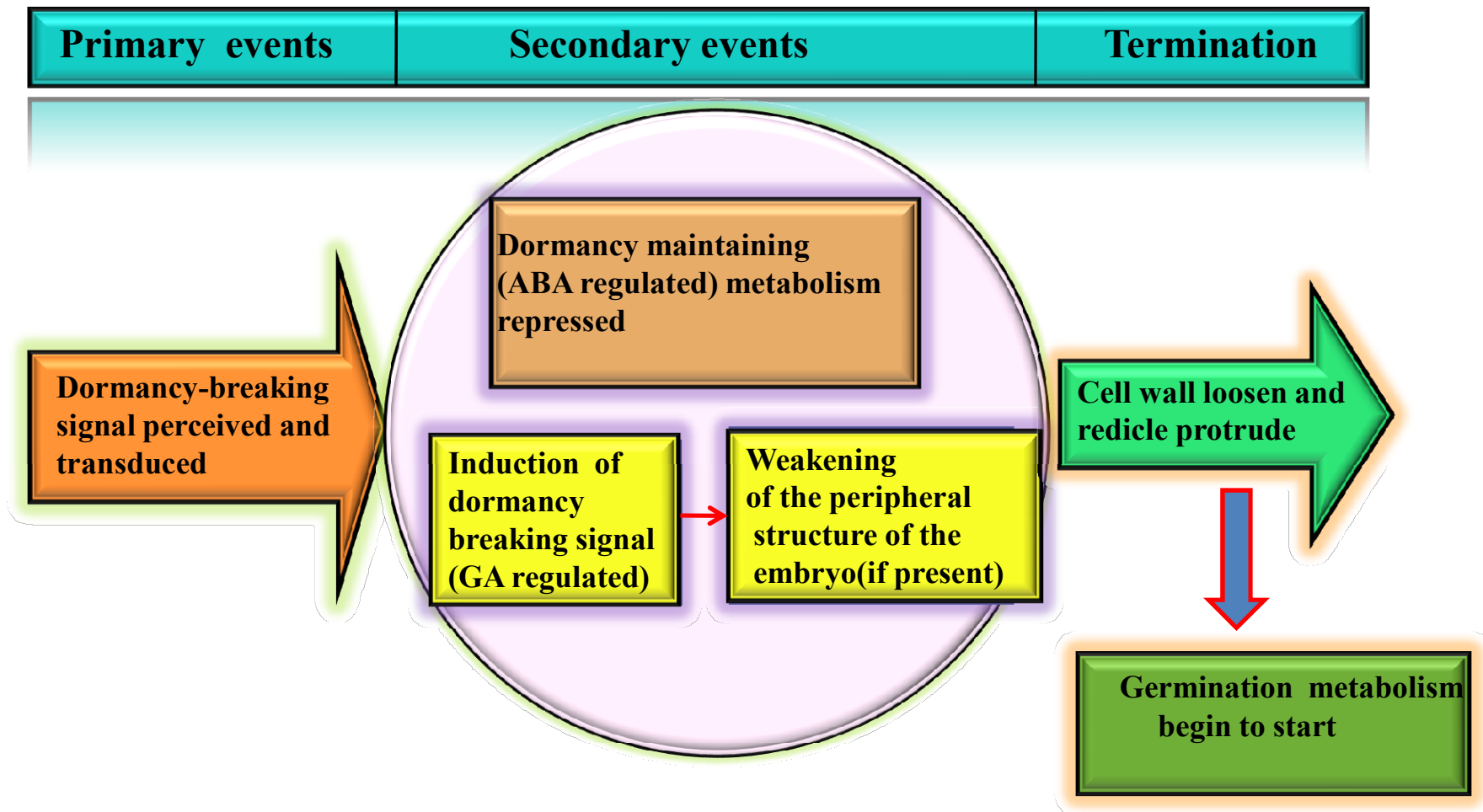


Figure 2.5. Major Events which are the integral part of breaking of Seed Dormancy (Image adapted from Bewley 1997 after modification).

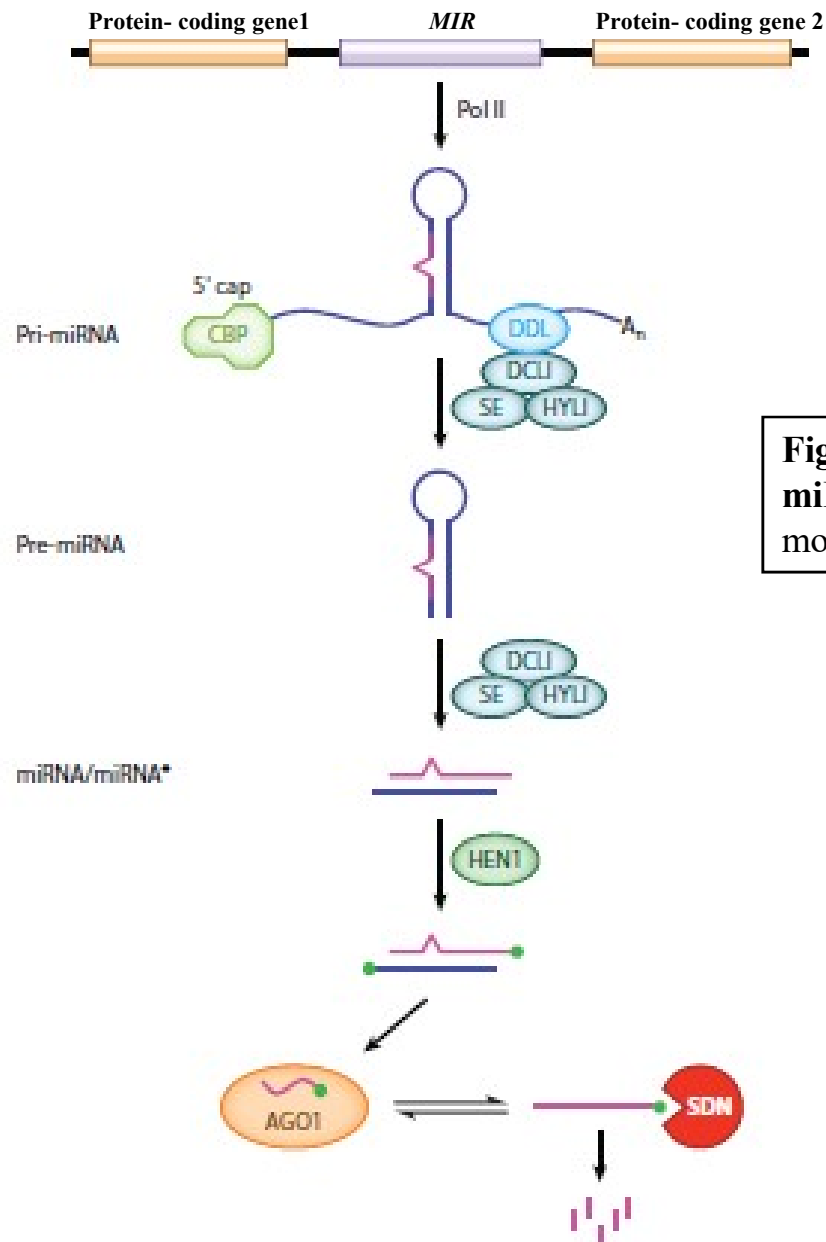


Figure 2.6 Diagrammatic representation of Plant miRNA biogenesis. [Image adapted with slight modification from (Chen, 2009)].

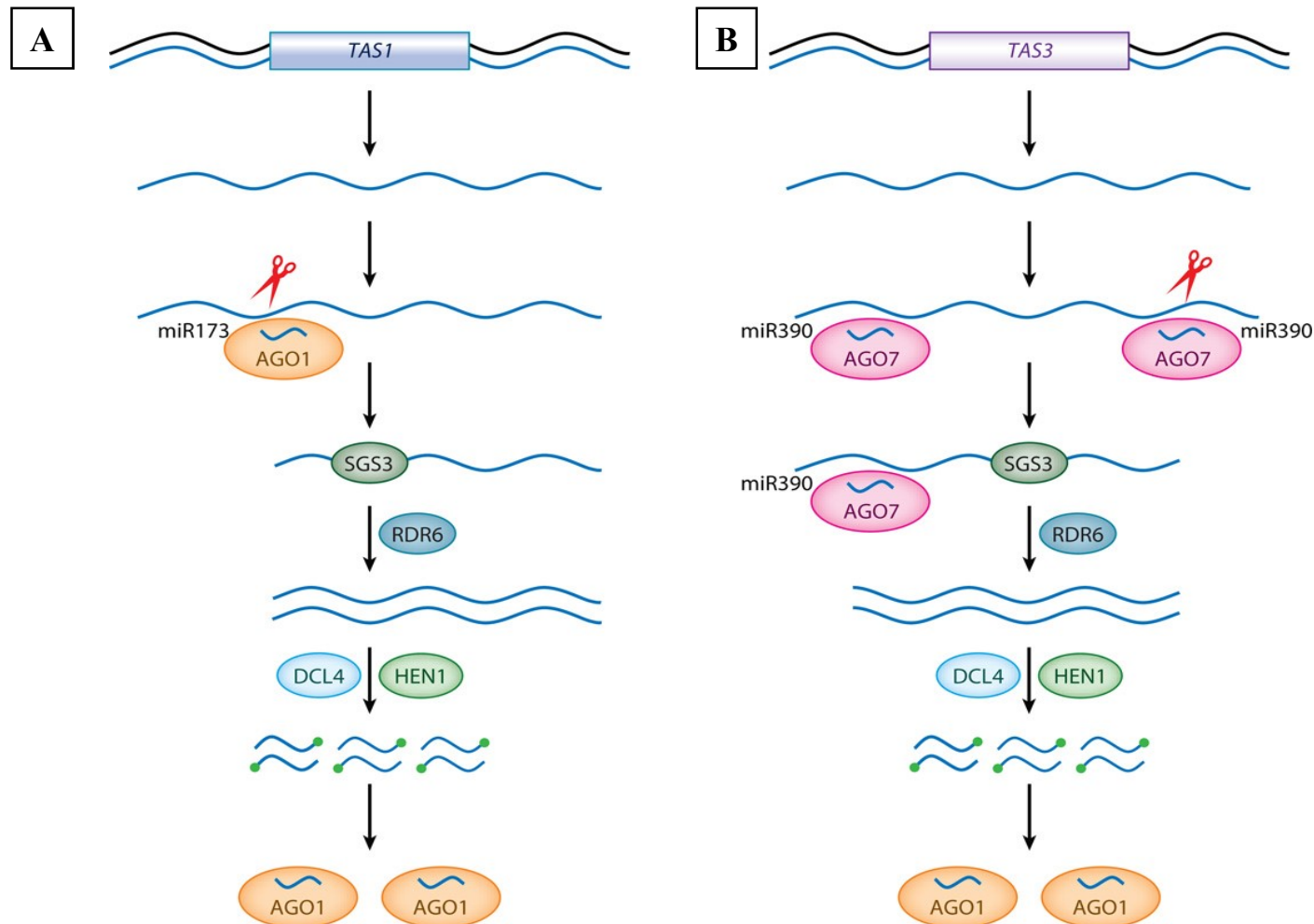


Figure 2.7 Diagrammatic representation of the biogenesis of Plant ta-siRNAs. (A) At the *TAS1* locus, long non coding precursor transcripts are cleaved by **miR173/AGO1**, and the 3' cleavage products are bound by **SGS3** and copied into dsRNAs by **RDR6**. The dsRNAs are further processed into siRNAs by **DCL4** in a step-wise manner from the end defined by the initial cutting/cleavage. **(B)** At the *TAS3* locus, long non coding precursor transcripts are recognized at two sites by **miR390/AGO7**, which cleaves the transcripts only at the 3' site. The 5' cleavage products are ultimately channellized into ta-siRNA production by **SGS3**, **RDR6**, and **DCL4** [Image adapted from (Chen, 2009)].

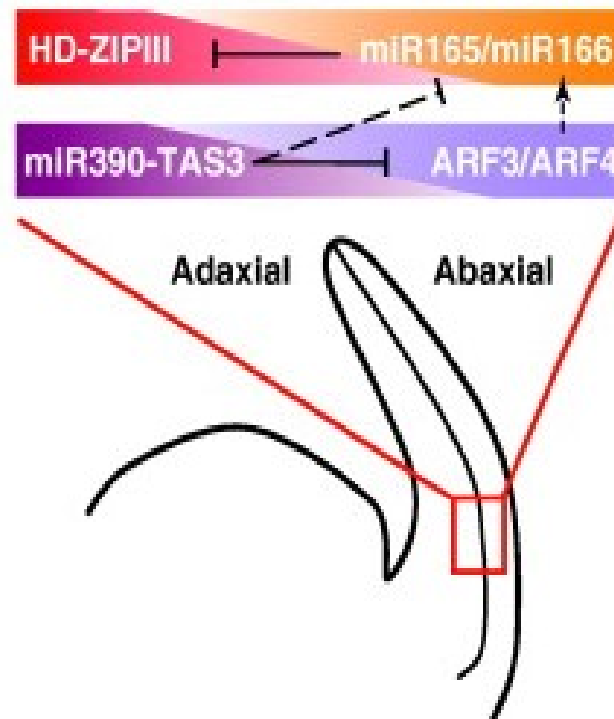


Figure 2.8 Interactions between miRNAs and their respective targets in determination of adaxial-abaxial leaf polarity. Black arrow indicates the positive regulation and the T-lines indicate the negative regulation. Dashed lines denote speculative behaviours and interactions [Image adapted from (Rubio-Somoza and Weigel, 2011)].

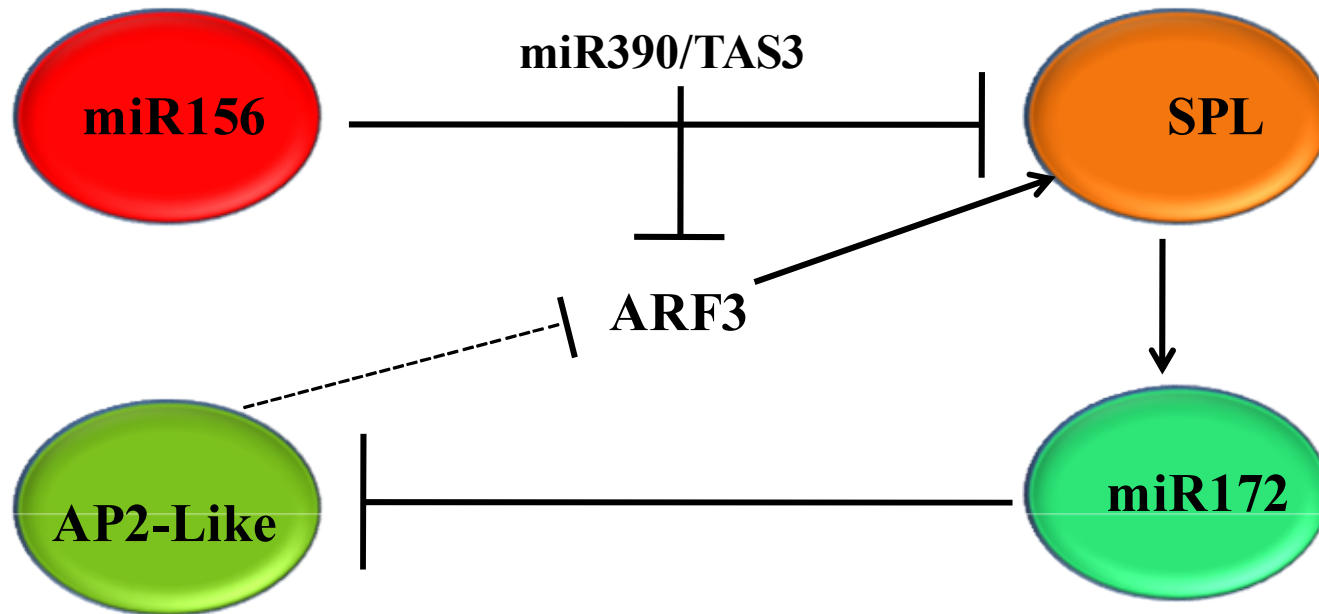


Figure 2.9 The interactions between miRNAs and their targets during developmental phase transition. **Solid black arrows** indicating positive regulation and **solid T-lines** indicating the negative regulation. Whereas the **dashed Lines** specify the speculative behaviours and interactions [Image adapted from (Rubio-Somoza and Weigel, 2011) after modification].

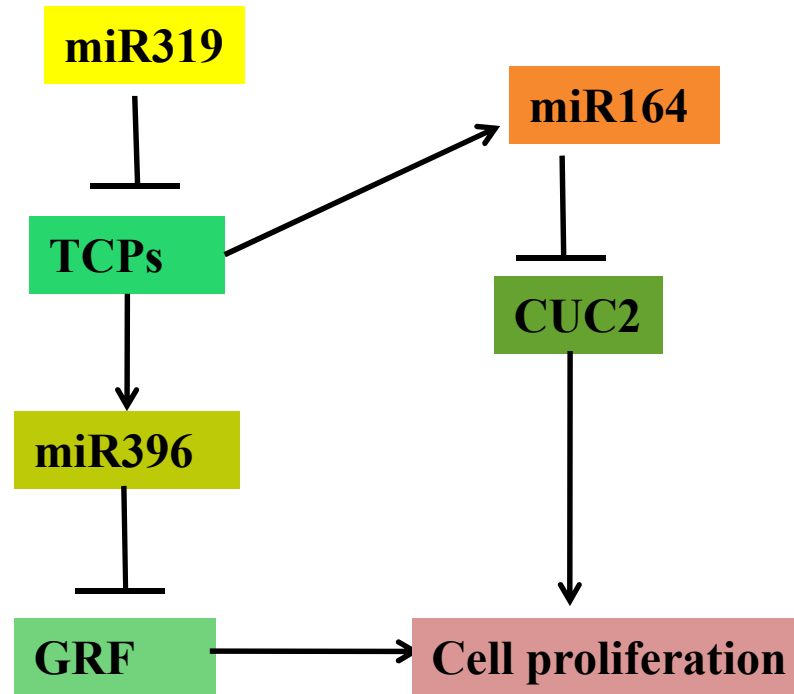


Fig 2.10. miRNAs and their target interactions regulating cell proliferation in leaves (Image adapted from (Rubio-Somoza and Weigel, 2011) after modification).

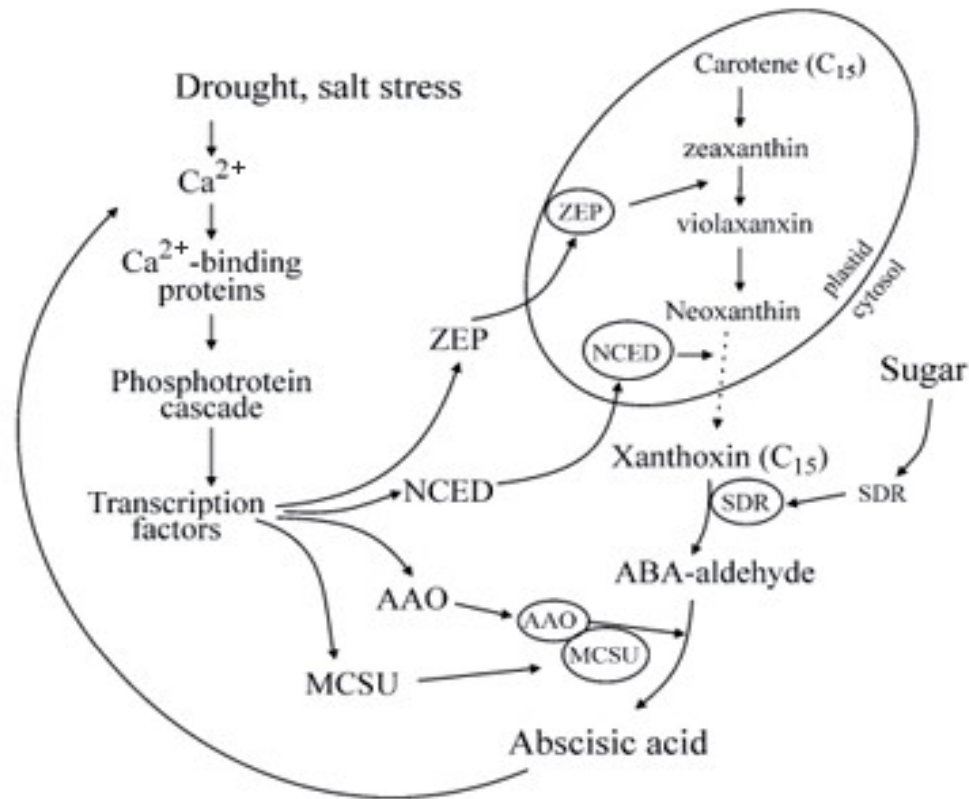


Fig 2.11 Biosynthetic pathway of ABA in higher plants. In plastids through an oxidative cleavage reaction from precursors C_{40} epoxy-carotenoid ABA is derived. In cytosol, the Xanthoxin (C_{15} intermediate) is converted to ABA after two-step reaction via ABA-aldehyde. Different abiotic stresses such as drought and salt activate the biosynthetic genes, most probably through a Ca^{2+} dependent cascade as shown on the left. ABA feedback excites the expression of the biosynthetic genes, which is also presumably through a Ca^{2+} dependent phosphoprotein series of interaction. Among several biosynthetic genes, *NCED* is strongly upregulated by abiotic stress whereas *SDR* is regulated by sugar. ABA biosynthetic genes are denoted with small ovals. The *NCED* step probably limits ABA biosynthesis in leaves (denoted with a dashed arrow). *NCED*: 9-cis-epoxycarotenoid dioxygenase; *ZEP*: zeaxanthin epoxidase; *MCSU*: MoCo sulfurase; *AAO*: ABA-aldehyde oxidase [Image adapted from (Xiong and Zhu, 2003)].

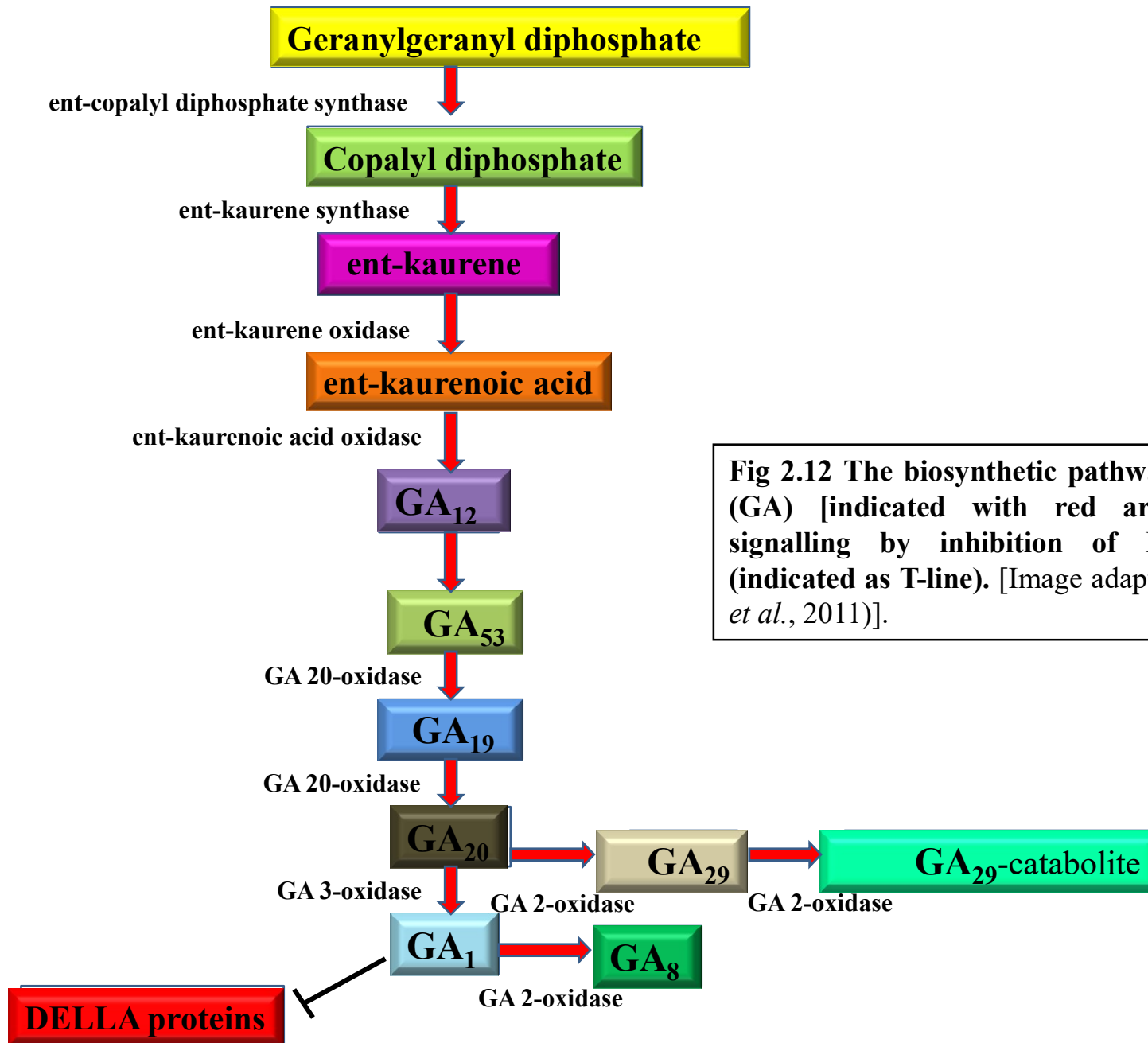


Fig 2.12 The biosynthetic pathway of Gibberellins (GA) [indicated with red arrow] and GA signalling by inhibition of DELLA proteins (indicated as T-line). [Image adapted from (Ferguson *et al.*, 2011)].

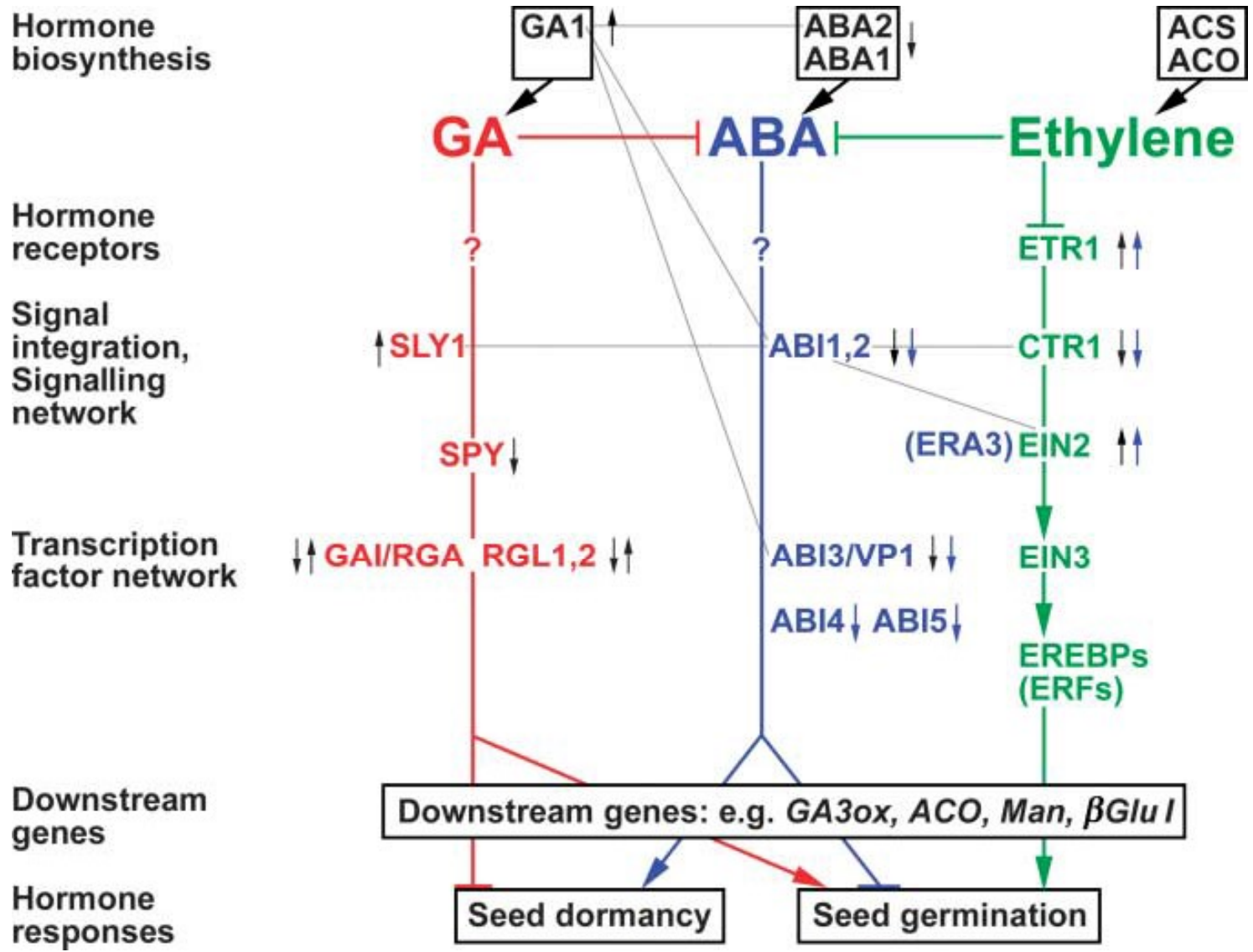


Fig 2.13

Fig 2.13 Diagrammatic representation of the interactions between the Abscisic acid (ABA), Gibberellin (GA) and Ethylene signalling pathways in the regulatory process of Seed Dormancy and Germination. This hypothetical model is mainly based on hormone mutant analyses in *Arabidopsis*. The interactions based on extranuclear enhancer or suppressor are indicated by thin grey lines. Interactions are indicated by thick arrows and blocks, respectively. Small black arrows specify the upregulation (upward arrow) or downregulation (downward arrow) of seed dormancy. Whereas small blue arrows specify increase (upward arrow) or decrease (downward arrow) of seed ABA sensitivity of the mutant of the corresponding proteins.

The shown hormonal mutant of *Arabidopsis thaliana* are : *rga* = repressor-of-gal-3; *rgl 1*, *rgl2* = *rga-like1*, 2; *aba1*, *aba2* = ABA-deficient1,2; *abi1* to *abi5* = ABA-insensitive1 to ABAinsensitive5; *era3* = enhanced response to ABA3; *ein2*, *ein3* = ethylene insensitive2, 3; *ctr1* = constitutive triple response1; *gai* = GA insensitive; *sly1* = sleepy1; *spy* = spindly;

Other abbreviations: **GA3ox** = GA 3-oxidase; **Man** = mannanase; **vp1** = viviparous1 (maize mutant); **EREBP** = ethylene responsive element binding protein; **ERF** = ethylene responsive factor; **ACS** = ACC synthase; **ACO** = ACC oxidase [Image adapted from (Kucera *et al.*, 2007)].

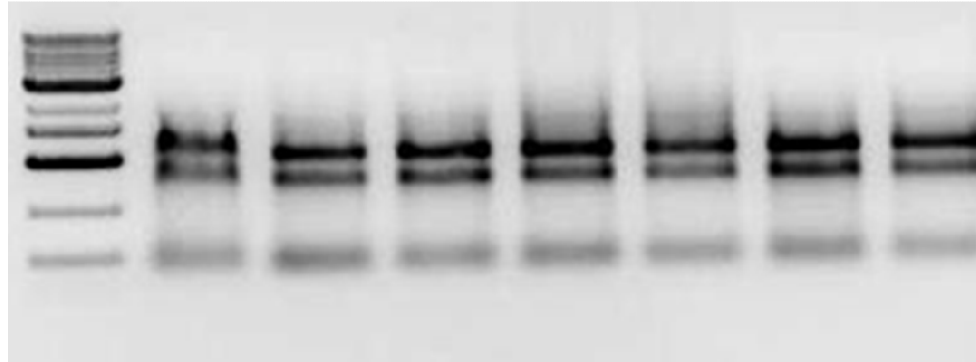


Figure 4.1.1 Total RNAs from *Arabidopsis* Wt Col seeds in TAE Agarose Gel (1.2%). [1- DS, 2-12h/RT, 3- 12h/4°C, 4-24h/RT, 5-24h/4°C, 6- 48h/RT, 7- 48h/4°C , (M)- marker].

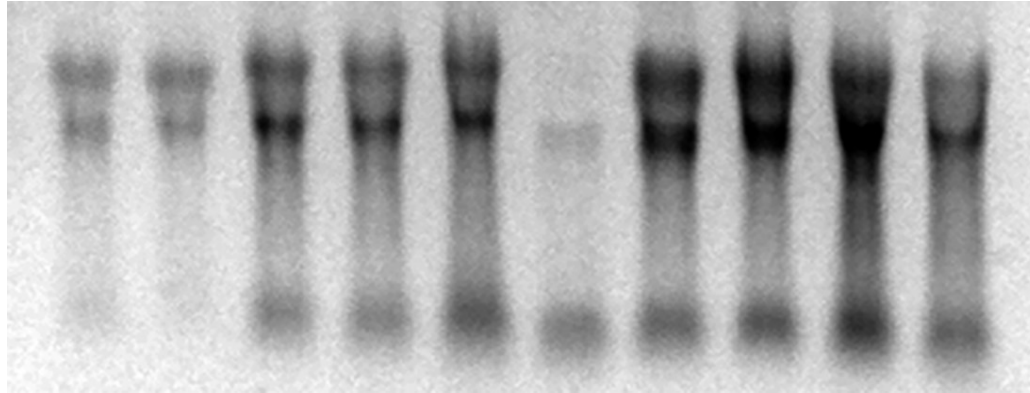


Figure 4.1.2 Total RNAs from *Arabidopsis* Wt Col seeds in MOPS-formaldehyde gel. [(A) and (B): Positive control RNAs from leaf and shoot tissues, (C): Empty lane having some RNA diffused into it from neighbouring well/s. 1- DS, 2-12h/RT, 3- 12h/4°C, 4- 24h/RT, 5-24h/4°C, 6- 48h/RT, 7- 48h/4°C

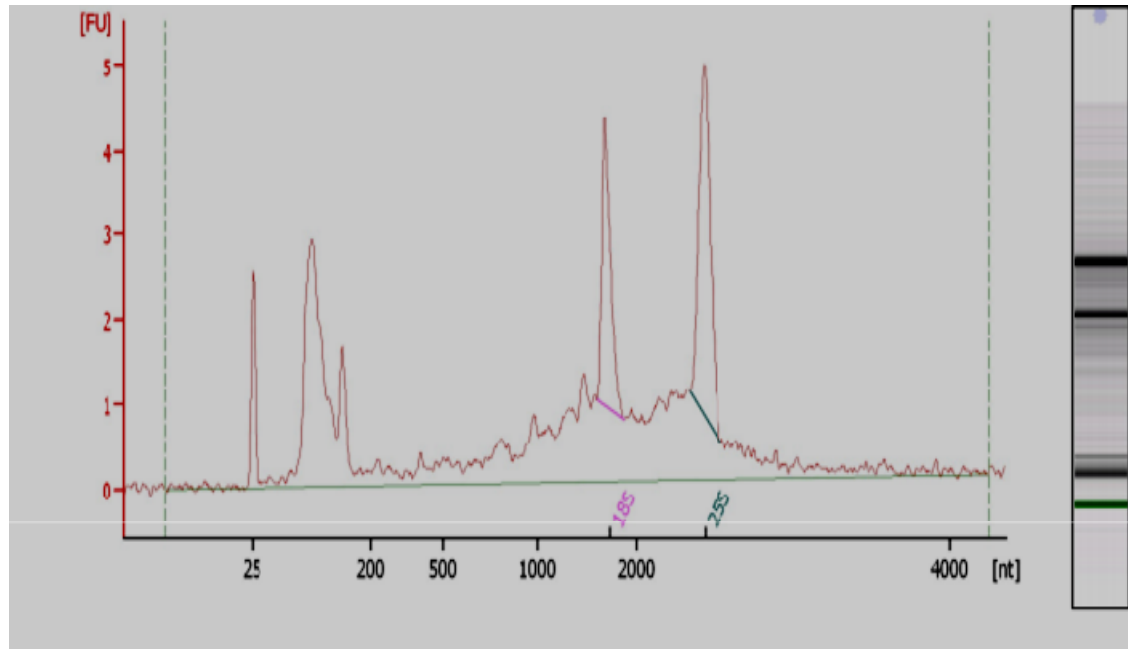


Figure 4.1.3 Quality of the RNA was checked by Bio-analyzer, showing RIN value-7.1 (almost each of the 7 above mentioned spatio-temporal conditions we obtained the same quality of RNAs).

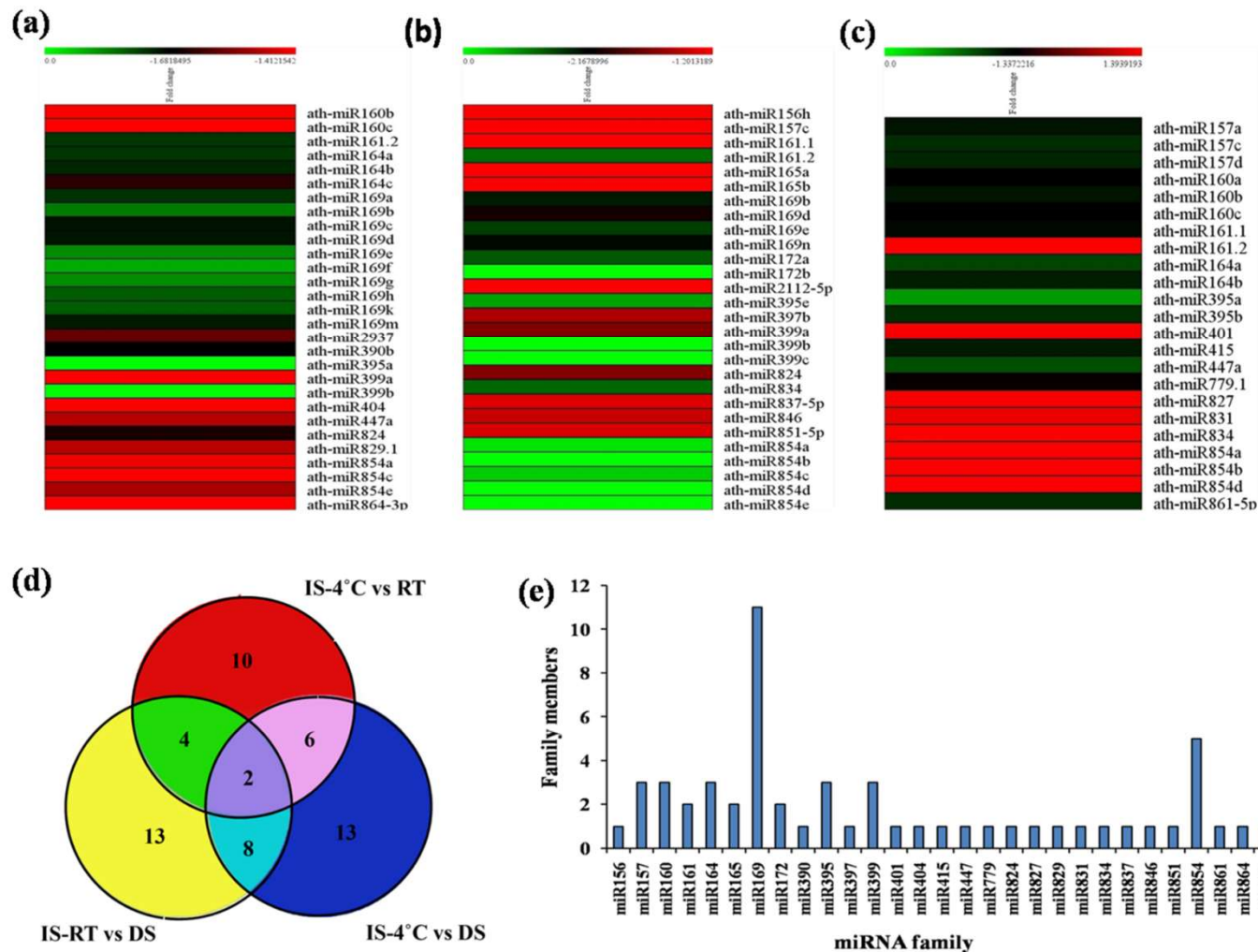


Figure 4.1.4 Expression patterns of miRNAs at different seed germination conditions in *Arabidopsis thaliana* based on Microarray . (a) Heat map analysis at Cold imbibitions (4°C) vs. Dry seeds (DS). (b) Heat map analysis at Room Temperature (RT) vs. Dry seed (DS). (c) Heat map analysis at Cold imbibitions (4°C) vs. Room temperature (RT). The bars in the heat map represent the scale of expression levels of the miRNAs. During Microarray we have pooled all the Cold imbibed (IS-4°C) and Room Temp imbibed (IS-RT) total RNAs separately, and the microarray was performed using two biological replicates for each individual samples. (d) The Venn diagram represents the comparison of the known miRNAs in between three different conditions (DS, IS-4°C and IS-RT) used in the Microarray Experiment. (e) The graph represents the miRNA families and their respective family members which were detected in our Microarray analysis. [For generating heat map we used MeV(Multiple Experiment Viewer) (<http://mev.tm4.org/>)].

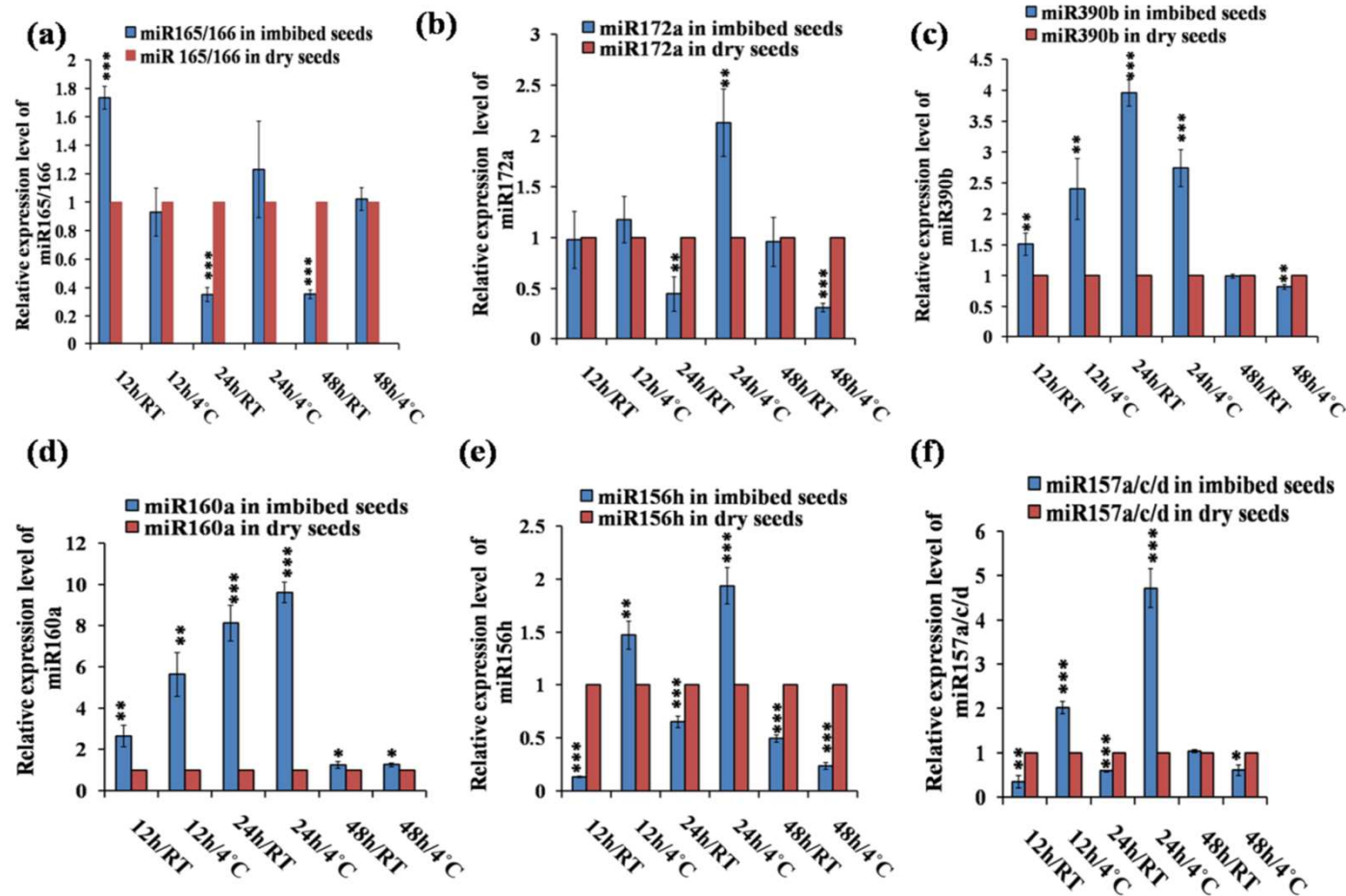


Figure 4.2.1 Quantitative RT-PCR based validation of the Expression of Mature miRNAs in Imbibed seeds, in comparison to Dry seeds, in *Arabidopsis thaliana*. (The Expression profiles generated upon qRT-PCR slightly varied with the miRNA expressions depending upon Microarray analysis, probably due to the pooling of total RNAs we used during Microarray experiment). The qRT-PCR validation of miRNAs were done at six different germination conditions as 12h/RT, 12h/4°C, 24h/RT, 24h/4°C, 48h/RT and 48h/4°C, each compared to Dry seed. The Expression values showed here representing the means of three biological replicates \pm standard deviation (sd). The *Arabidopsis ACTIN7* was used for each samples as an Endogenous control. (a) ath-miR165/166; (b) ath-miR172a; (c) ath-miR390b; (d) ath-miR160a; (e) ath-miR156h; (f) ath-miR157a/or, c/or, d. In *Arabidopsis*, miR157a, c and d have the same mature sequence. Asterisks indicate significant statistical differences: ***P < 0.001, **P < 0.01, *P < 0.05 [One-way ANOVA].

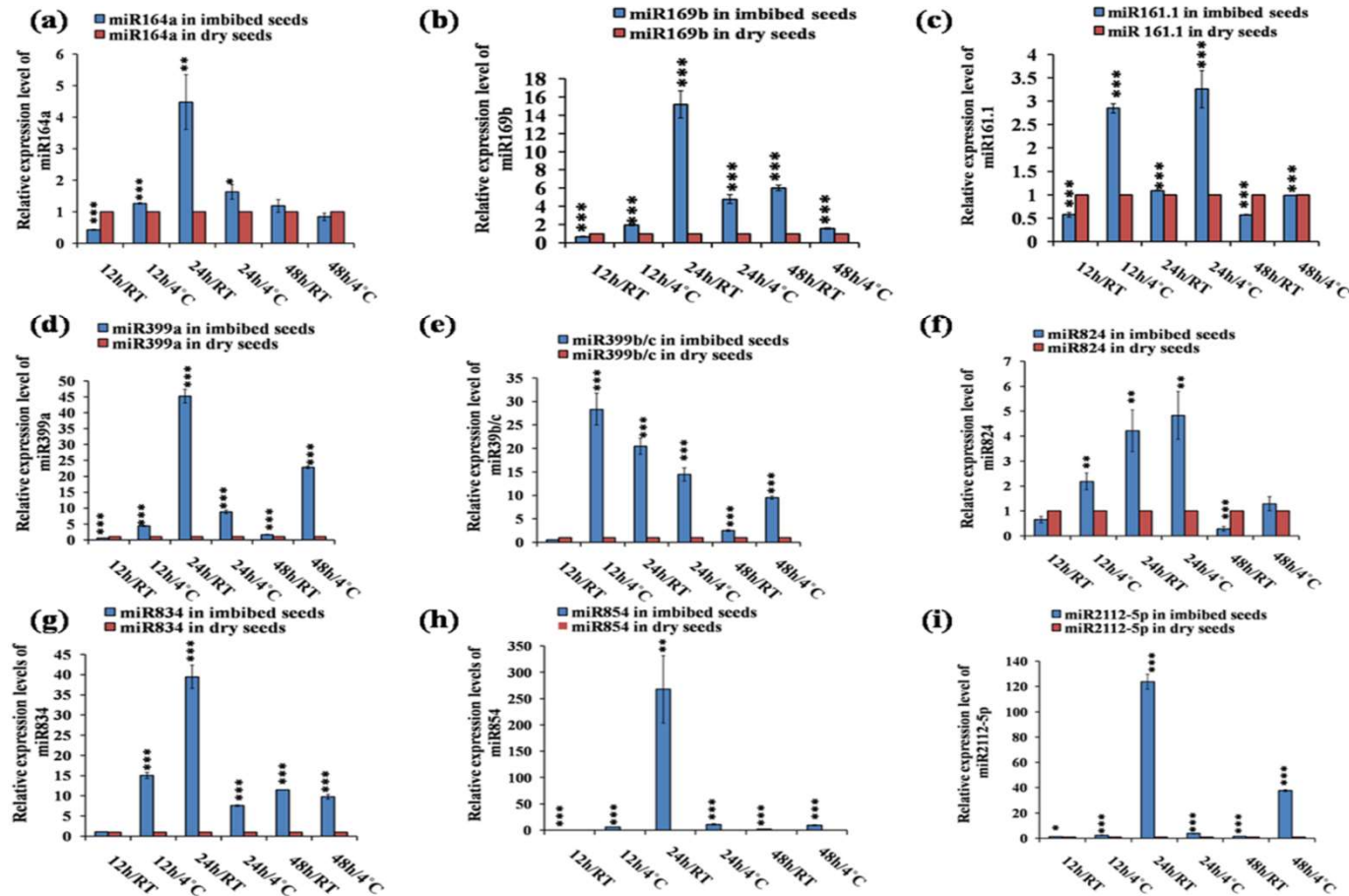


Figure 4.2.2 The validation of Expression of Mature miRNAs in imbibed seeds, in comparison to Dry seeds, in *Arabidopsis thaliana* by quantitative RT-PCR method. The qRT-PCR validation of miRNAs were done at six different Germination conditions as 12h/RT, 12h/4°C, 24h/RT, 24h/4°C, 48h/RT and 48h/4°C each compared to Dry seed. The Expression values showed here representing the means of three biological replicates \pm standard deviation (sd). The *Arabidopsis ACTIN7* was used for each samples as an Endogenous control. (a) ath-miR164a; (b) ath-miR169b; (c) ath-miR161.1; (d) ath-miR399a; (e) ath-miR399b/or, c (in *Arabidopsis*, miR399b and c have the same mature sequences); (f) ath-miR824; (g) ath-miR834; (h) ath-miR854; (i) ath-miR2112-5p. Here Asterisks indicate significant statistical differences: ***P < 0.001, **P < 0.01, *P < 0.05 [One-way ANOVA].

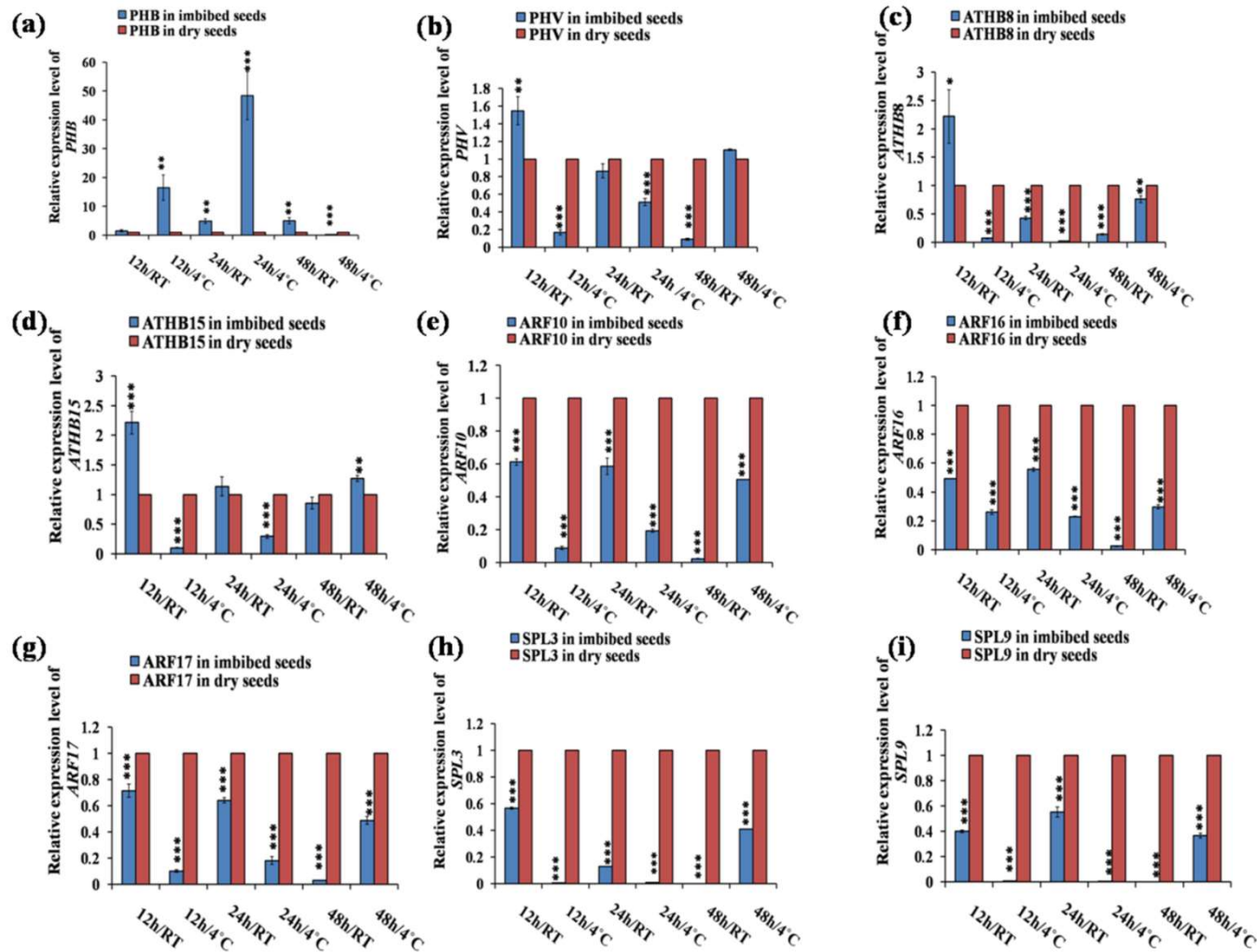


Figure 4.2.3 Validation of the Expression of Mature miRNAs in imbibed seeds, in comparison to Dry seeds, in *Arabidopsis thaliana* by quantitative RT-PCR method. The qRT-PCR validation of miRNAs were done at six different Germination conditions as 12h/RT, 12h/4°C, 24h/RT, 24h/4°C, 48h/RT and 48h/4°C each compared to Dry seed. The Expression values showed here representing the means of the three biological replicates \pm standard deviation (sd). The *Arabidopsis ACTIN7* was used for each samples as an Endogenous control. (a-d) targets of miR165/166; (a) *PHB*; (b) *PHV*; (c) *ATHB8*; (d) *ATHB15*. (e-g) targets of miR160; (e) *ARF10*; (f) *ARF16*; (g) *ARF17*. (h-i) targets of miR156/ or, miR157; (h) *SPL3*; (i) *SPL9*. Here Asterisks indicate significant statistical differences, ***P < 0.001, **P < 0.01, *P < 0.05 [One-way ANOVA].

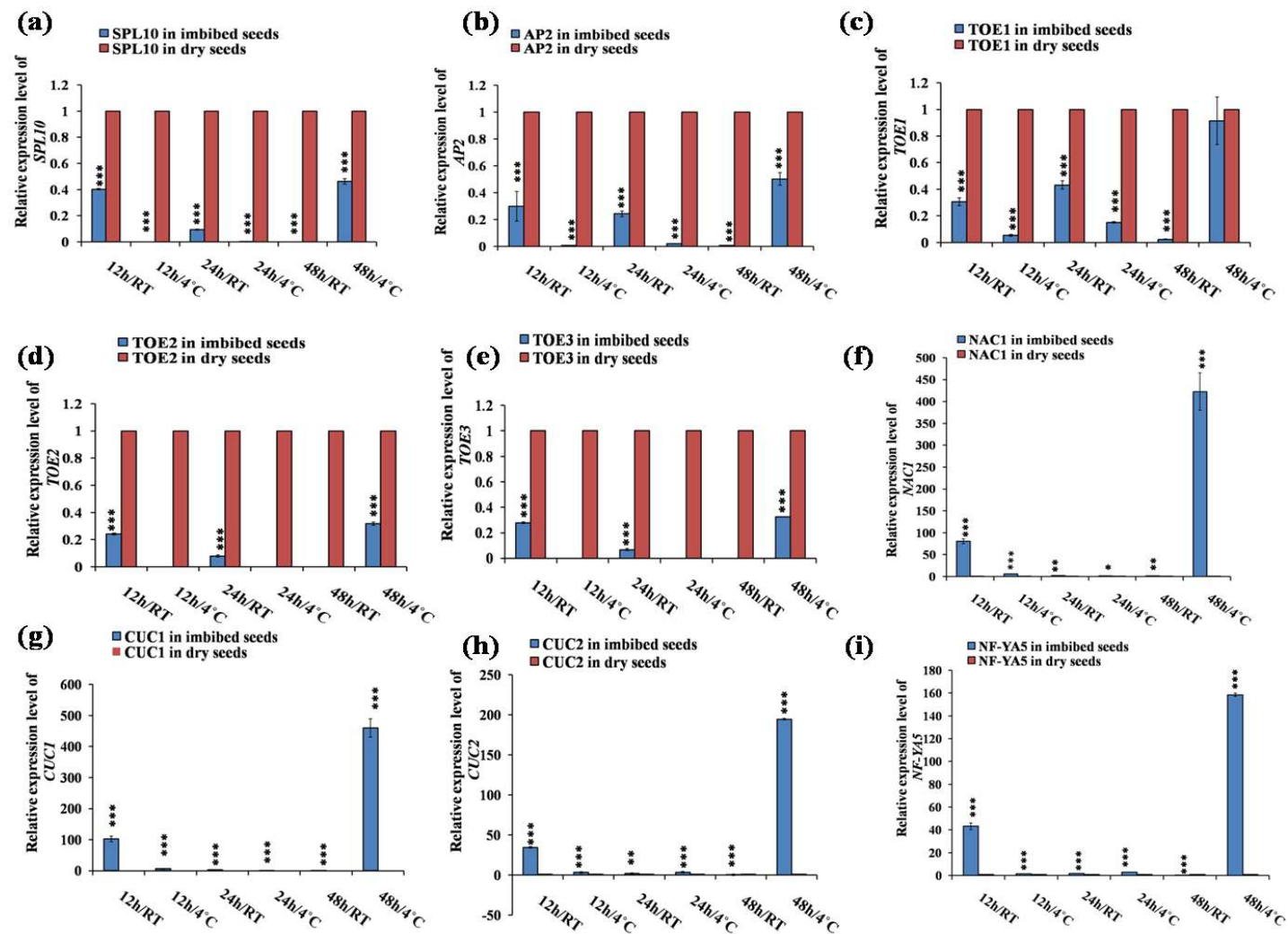


Figure 4.2.4 Validation of the Expression of Mature miRNAs in imbibed seeds, in comparison to Dry seeds, in *Arabidopsis thaliana* by quantitative RT-PCR method. The qRT-PCR validation of miRNAs were done at six different Germination conditions as 12h/RT, 12h/4°C, 24h/RT, 24h/4°C, 48h/RT and 48h/4°C each compared to Dry seed. The Expression values showed here representing the means of the three biological replicates \pm standard deviation (sd). The *Arabidopsis ACTIN7* was used for each and every samples as an Endogenous control. (a) SPL10- target of miR156/or, miR157. (b–e): targets of miR172; (b) AP2; (c) TOE1; (d) TOE2; (e) TOE3. (f–h): targets of miR164; (f) NAC1; (g) CUC1; (h) CUC2; (i) NF-YA5- target of miR169. Here Asterisks indicate significant statistical differences; ***P < 0.001, **P < 0.01, *P < 0.05 [One-way ANOVA].

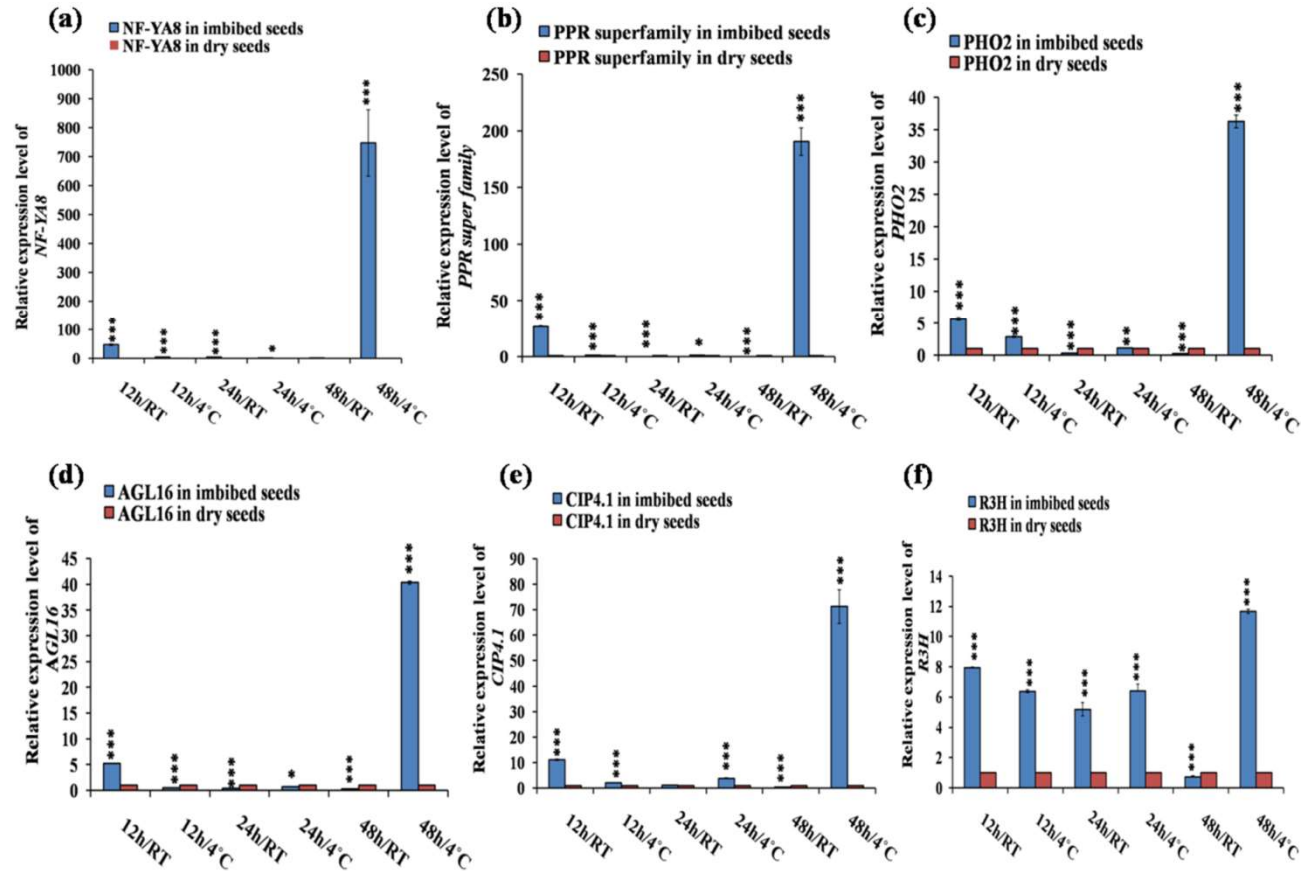


Figure 4.2.5 Validation of the Expression of Mature miRNAs in imbibed seeds, in comparison to Dry seeds, in *Arabidopsis thaliana* by quantitative RT-PCR method. The qRT-PCR validation of miRNAs were done at six different Germination conditions as 12h/RT, 12h/4°C, 24h/RT, 24h/4°C, 48h/RT and 48h/4°C each compared to Dry seed. The Expression values showed here representing the means of the three biological replicates \pm standard deviation (sd). The *Arabidopsis ACTIN7* was used for each and every samples as an Endogenous control. (a) *NF-YA8*-target of miR169; (b) *PPR superfamily*- target of miR161.1; (c) *PHO2*- target of miR399; (d) *AGL16*- target of miR824; (e) *CIP4.1* or *CIP4*- target of miR834; (f) *R3H*- target of miR854. Here Asterisks indicate significant statistical differences; ***P < 0.001, **P < 0.01, *P < 0.05 [One-way ANOVA].

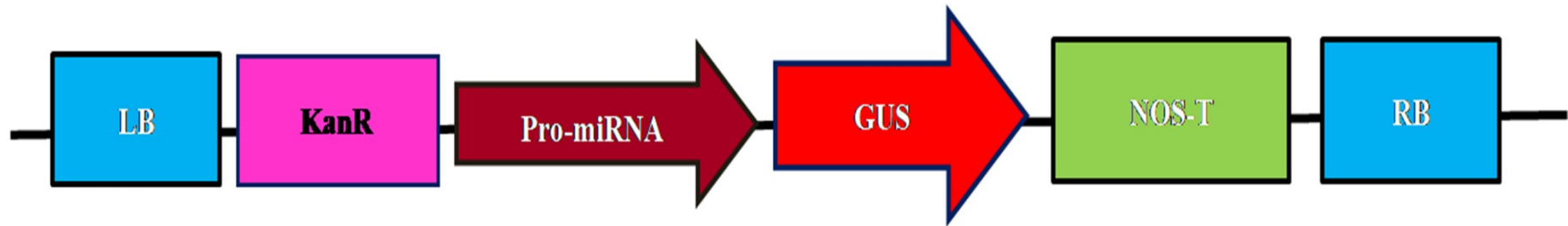


Figure 4.2.6. *pMIR390b::GUS* and *pMIR160a::GUS* construction

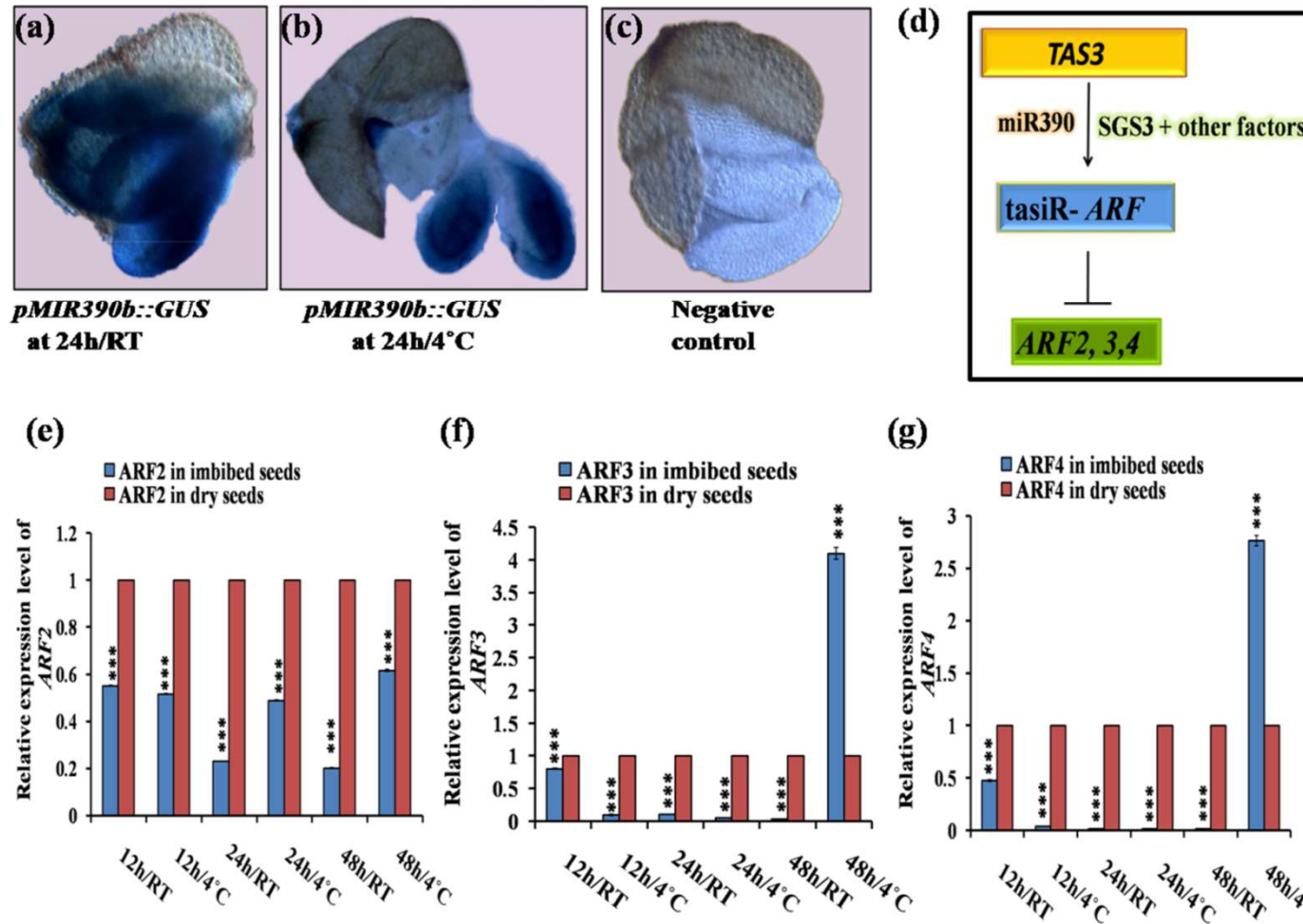


Figure 4.2.7 The Spatial Expression of *pMIR390b::GUS* in Germinating Seeds, the Function of miR390, and the Expression of the targets *ARF2*, *ARF3*, and *ARF4* during Seed Germination. (a) *GUS* Expression of *pMIR390b::GUS* at 24h/RT Imbibed condition; (b) *GUS* Expression of *pMIR390b::GUS* at 24h/4°C Imbibed condition; (c) Negative control of *GUS* assay at 24h/ 4°C Imbibed Col-0 seed. 24h/RT-Imbibed seeds were showing the higher expression of miR390b compare to 24h/4°C-Imbibed seeds, which is matching or similar to the Expression pattern of the qRT-PCR based validation result of miR390b; (d)The model representing the role of miR390 in the biogenesis of tasiR-ARFs and regulation of *ARF2/3/4* (According to Marin et al, 2010). (e-g) Expression pattern of *ARF2/3/4* (the targets of tasiR-ARF) by qRT-PCR method; (e) Transcript level of target *ARF2*; (f) Transcript level of target *ARF3* and (g) Transcript level of target *ARF4*.

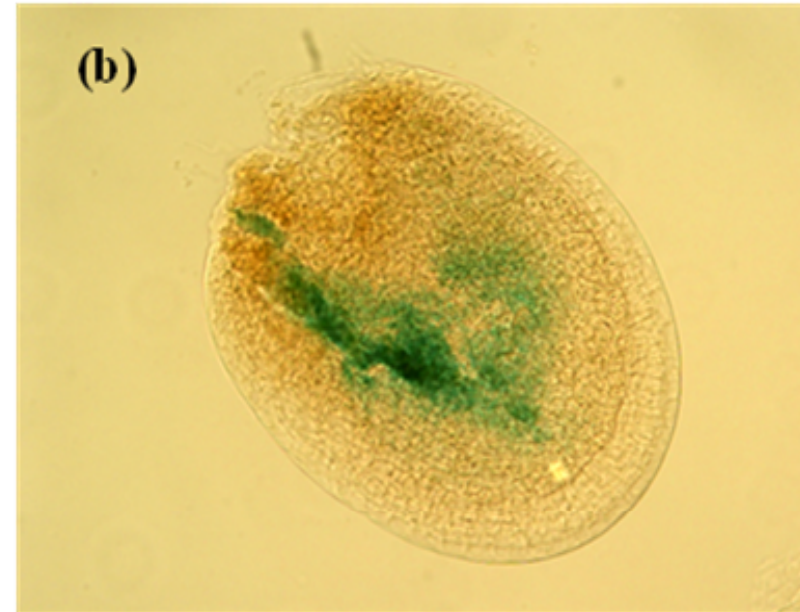
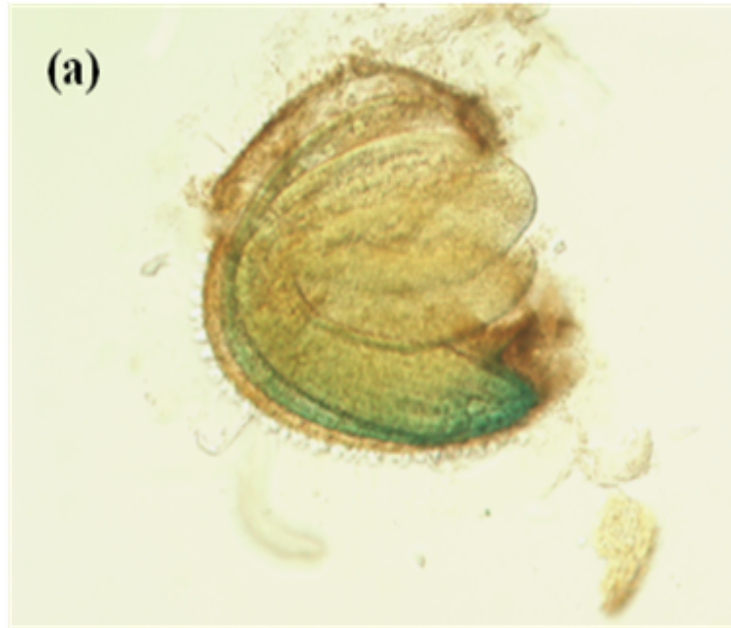


Figure 4.2.8. Spatial expression of *pMIR160a::GUS* in germinating seeds . (a). *GUS* expression in radicle at 12h/RT ; (b). *GUS* expression in endosperm at 12h/RT.

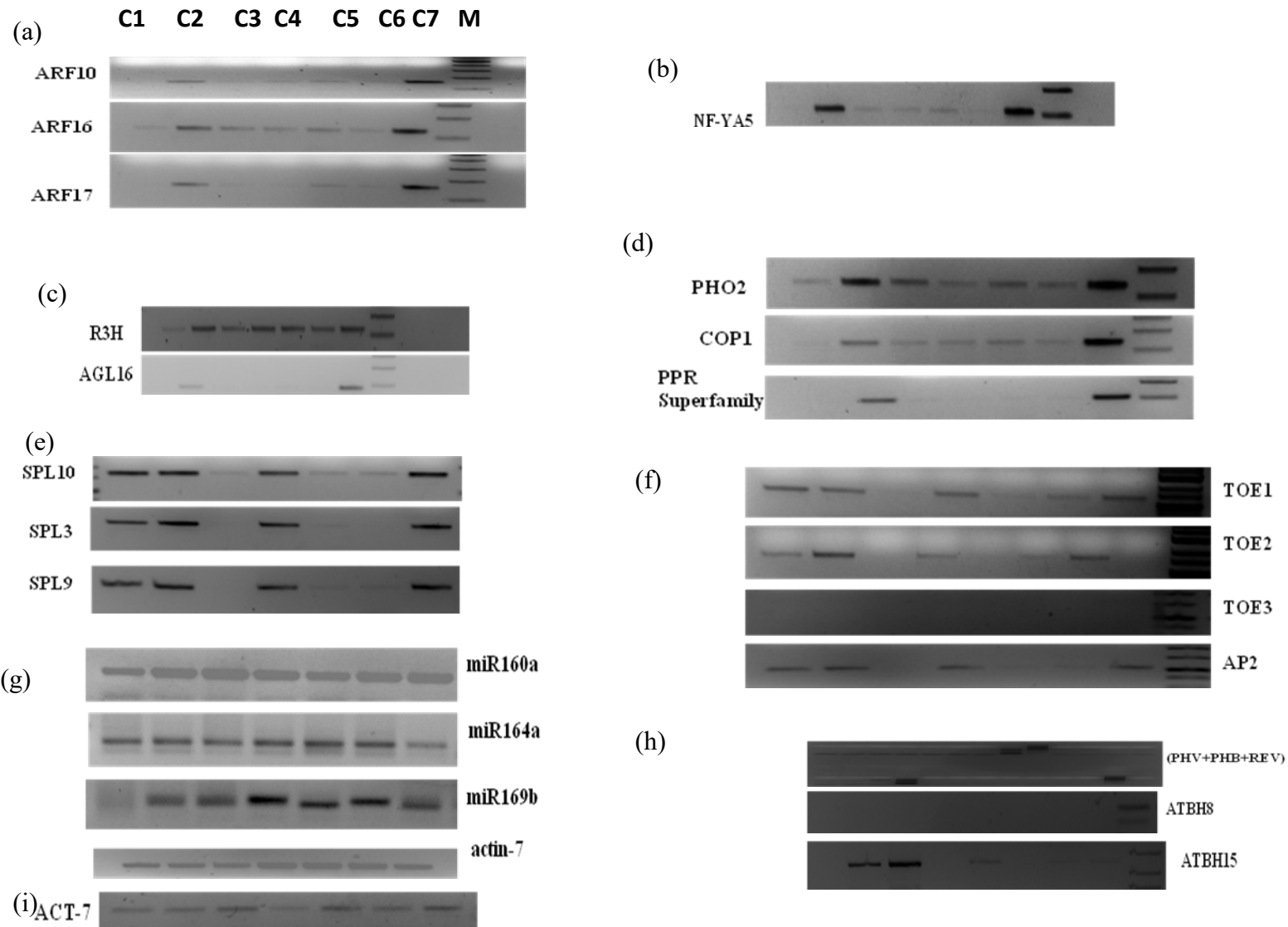


Figure 4.2.9(a-i). Semi quantitative RT-PCR of the targets and miRNAs (all are not shown). *ACT7* was an endogenous control. C1-Dry seed, C2- 12h/RT, C3-12h/4°C, C4-24h/RT, C5-24h/4°C, C6-48h/RT, C7-48h/4°C, M-marker

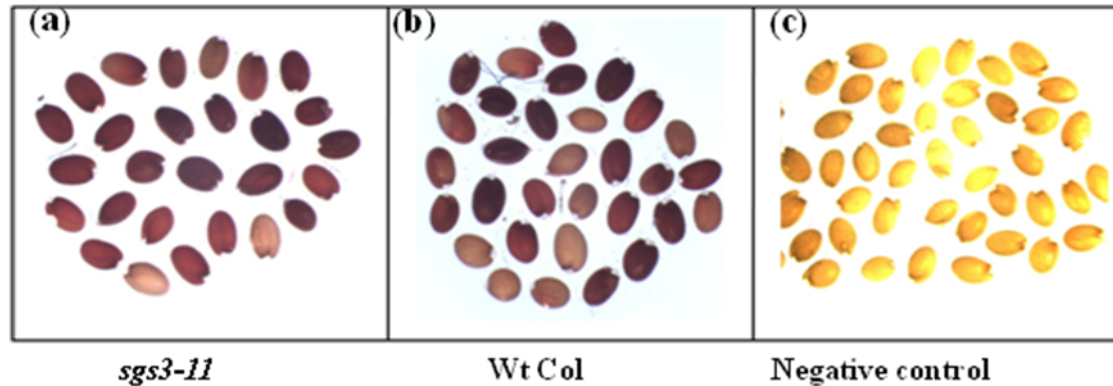


Figure 4.3.1. Tetrazolium assay of small RNA biogenesis pathway mutant *sgs3-11* seeds along with its age matched control Wt-Col seeds. The assay was performed in triplicate in both the cases. The Brown/or, red/or, dark brown colored seeds were viable seeds, less bright colored seeds were comparatively less viable, and the yellow colored seeds were non-viable(heat killed); **(a).** *sgs3* mutant seeds, **(b).** Positive control wt-col seeds; **(c).** Negative control (heat killed wt-col seeds).

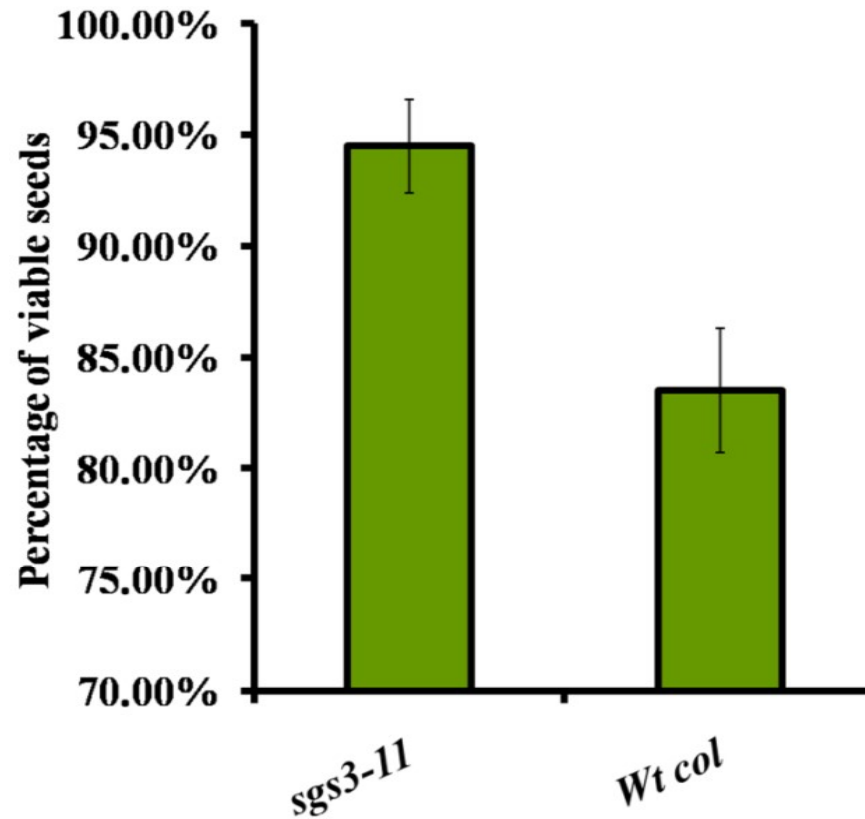


Figure 4.3.2. Relative percentage level of the viable seeds in both *sgs3-11* and Wt-Col ; the percentage was calculated based on the viable seeds of tetrazolium assay. The whole experiment was repeated at least three times along with the three set of independent lines of seeds.

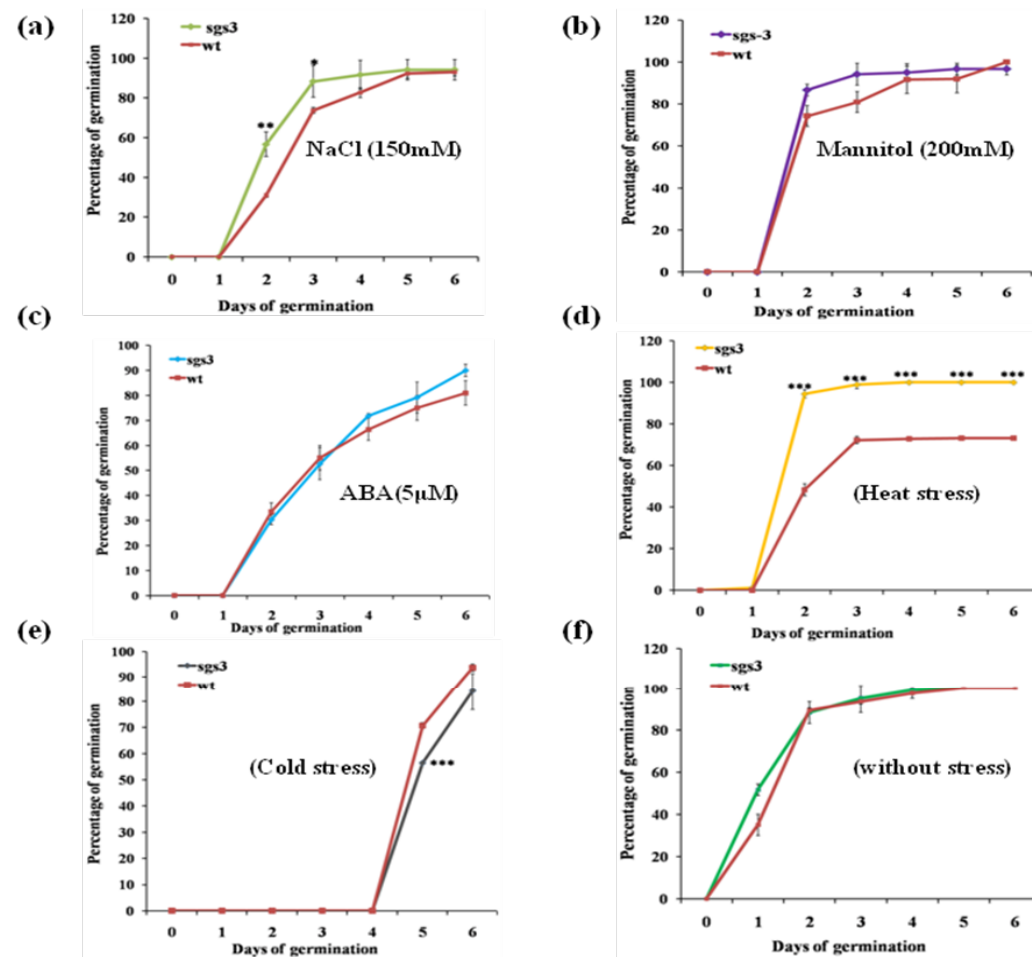


Figure 4.3.3. Germination assay of small RNA biogenesis pathway mutant *sgs3-11* seeds under abiotic stresses. (a). Salt (150mM NaCl), (b). Dehydration (mannitol, 200mM), (c). ABA (5µM), (d). Heat (45°C), (e). Cold (4°C), (f). Control condition (without stress). Age matched seeds were surface sterilized and plated on either 1/2 MS or 1/2 MS supplemented with various stresses. Plates were stratified at 4°C for 3 days and transferred to growth chamber at 22±2°C. For cold stress, after stratification plates were transferred to cold room (4°C) under 16/8h light/dark cycle till 4 days. Then transferred to again growth chamber at 22±2°C. Values are mean ±SD of three independent sets (n=30). Asterisks indicate significant statistical differences, ***P < 0.001, **P < 0.01, *P < 0.05 (One-way ANOVA).

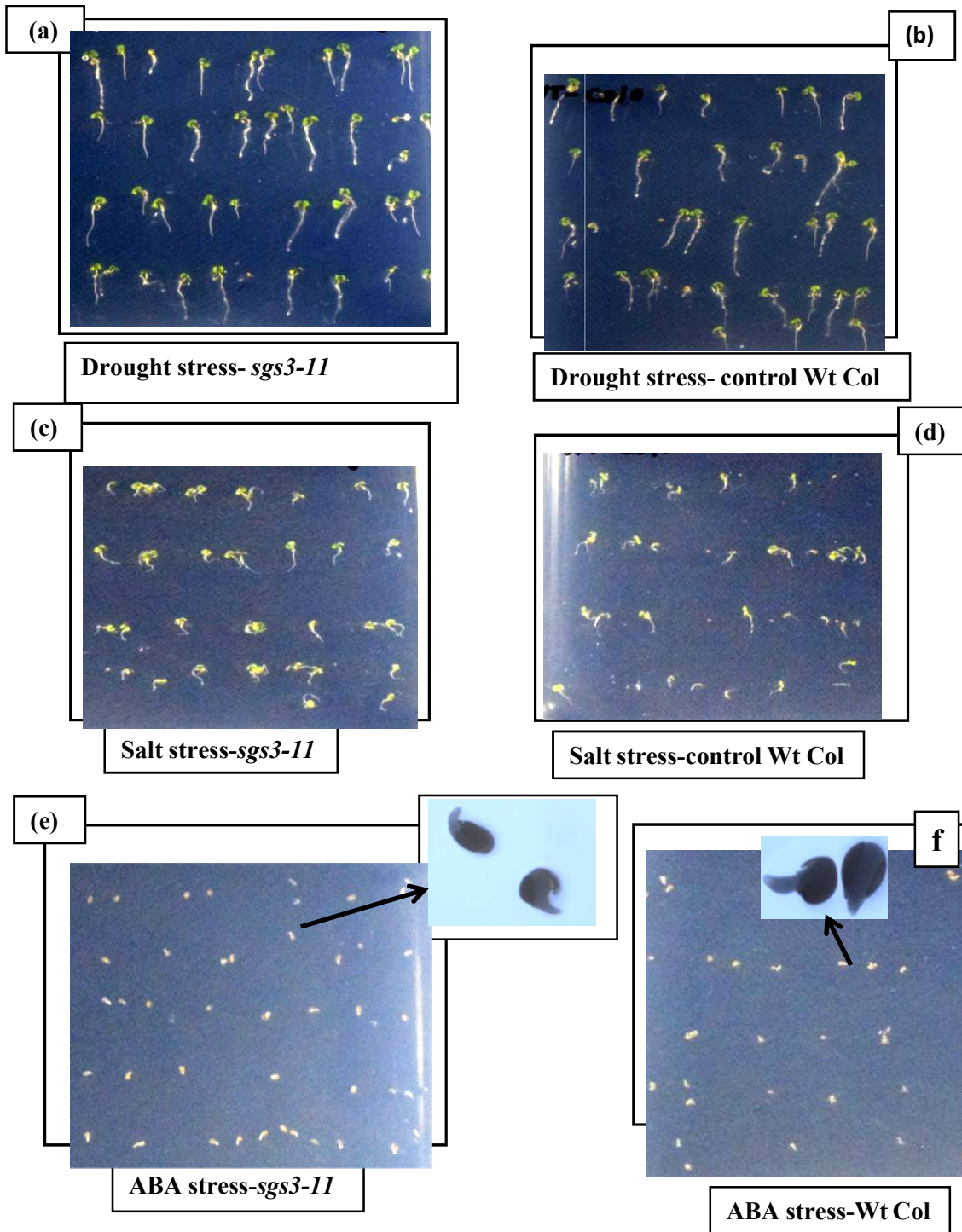
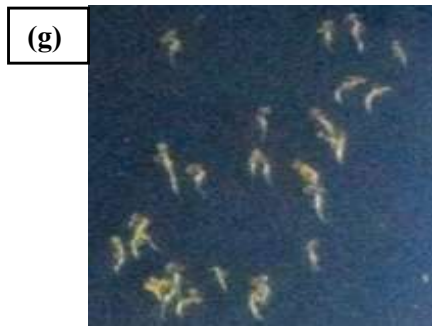


Figure 4.3.4. Effect of different stresses on germination of *sgs3-11* mutant seeds along with its control Wt Col on 4th day of germination (DAG4). (a, b) – Drought stress (mannitol (200mM), (c, d)- Salt stress (NaCl (150mM), (e, f)- Hormonal stress (ABA (5µM), (g, h)- Heat stress (45°C), (i, j)- Cold stress. Rate of germination in the respective stress conditions are calculated in Fig. 4.3.2.3.



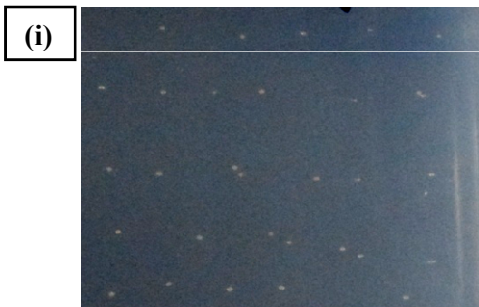
(g)

Heat stress- *sgs3-11*



(h)

Heat stress-Wt Col



(i)

Cold stress- *sgs3-11*

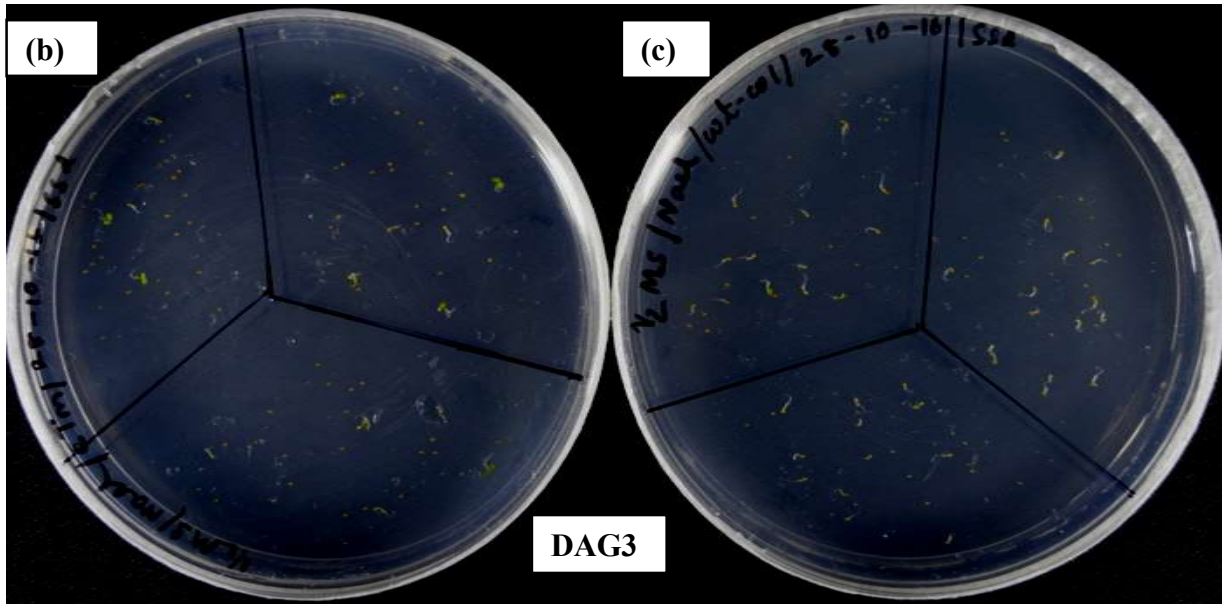
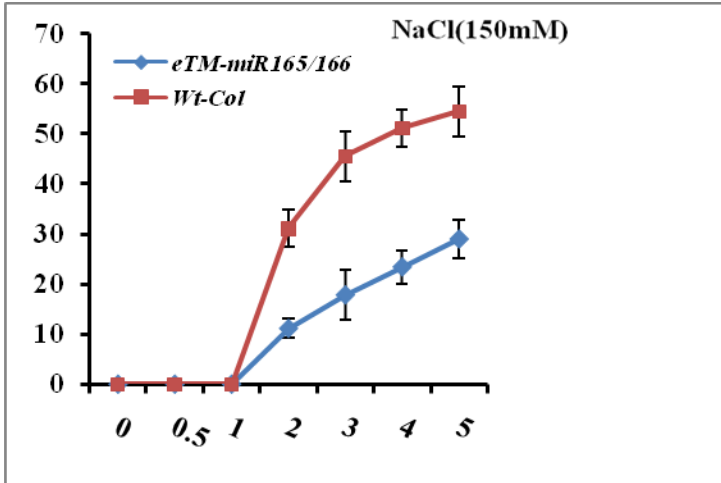


(j)

Cold stress-Wt Col

Figure- 4.3.4

(a)



(d)



(e)

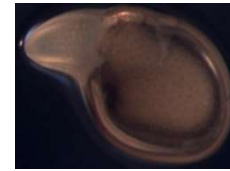
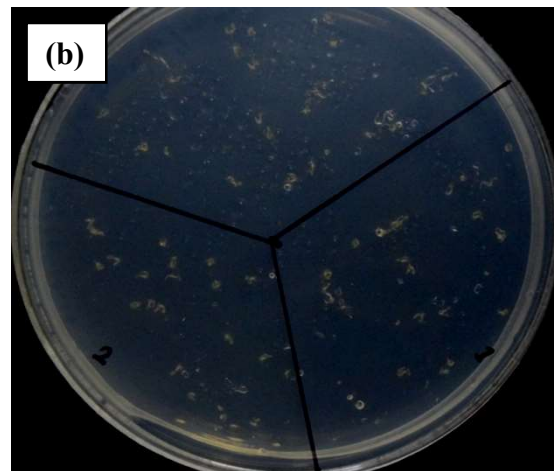
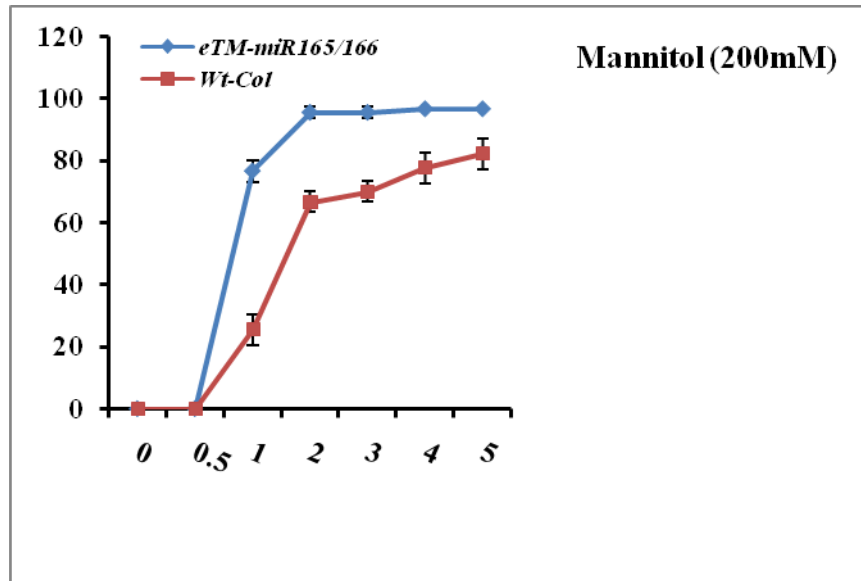
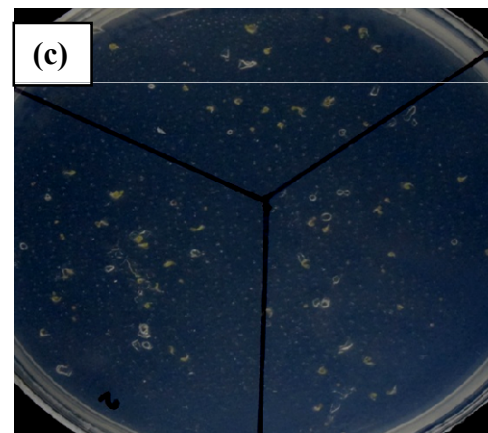


Figure 4.4.1. Effect of salt treatment on seed germination of the *eTM-miR165/166* and wild type plants. (a). Rate of germination of the *eTM-miR165/166* and wild type was measured in the medium supplemented with 150mM NaCl. And the germination scored at indicated days. (b), (c) Germination phenotype of *eTM-miR165/166* and wild type seeds in the media supplemented with salt respectively 3rd day after germination (DAG3). (d),(e) Radicle growth of *eTM-miR165/166* and Wt Col respectively after 3rd day of germination under stereozoom microscope.



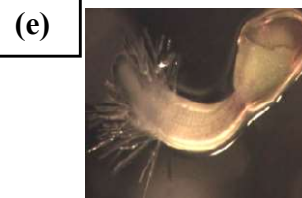
eTM-miR165/166



Wt Col



eTM-miR165/166



Wt Col

Figure 4.4.2. Effect of draught stress on seed germination of the *eTM-miR165/166* and wild type plants. (a). Rate of germination of the *eTM-miR165/166* and wild type was measured in the medium supplemented with 200mM mannitol. And the germination scored at indicated days. (b) and (c). Germination phenotype of *eTM-miR165/166* and wild type seeds in the media supplemented with mannitol respectively 3rd day after germination (DAG3). (d) and (e). Growth of *eTM-miR165/166* and Wt Col germinated seeds respectively after 3rd day of germination under steriozoom microscope.

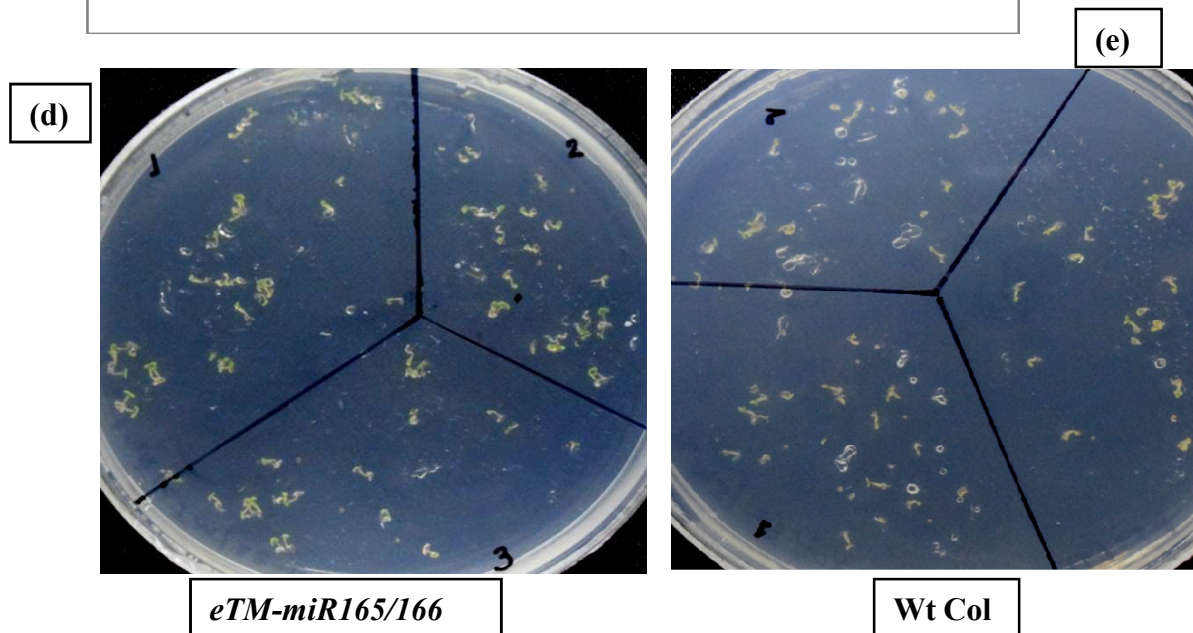
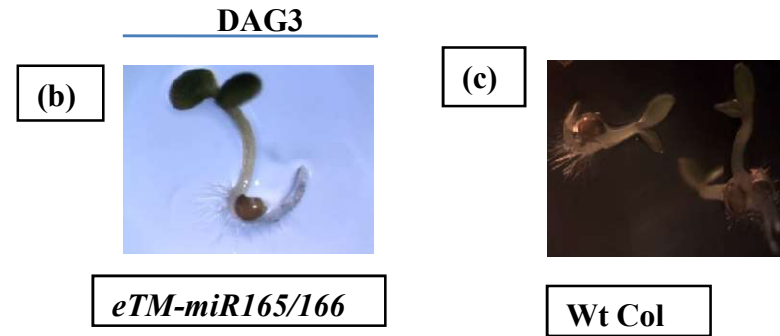
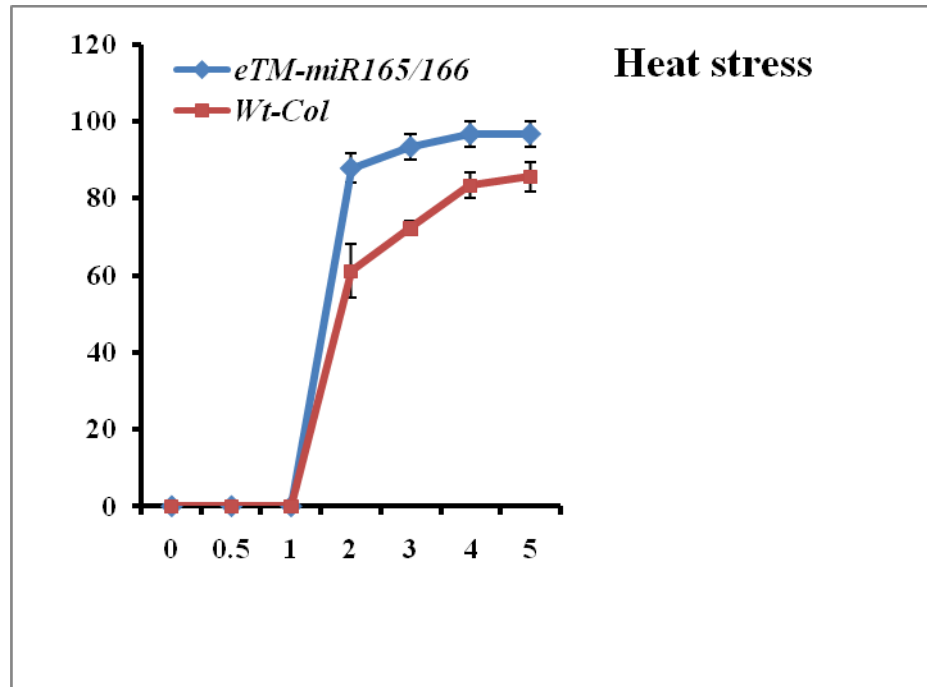
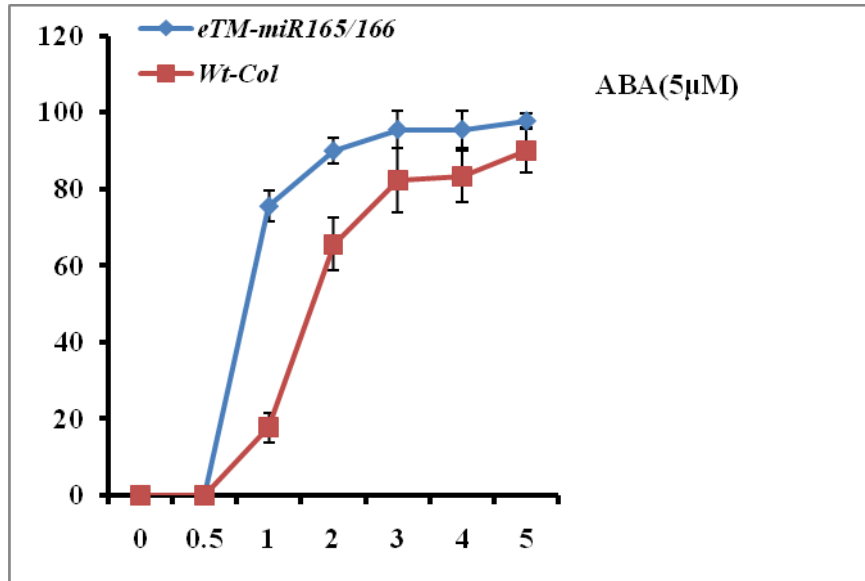


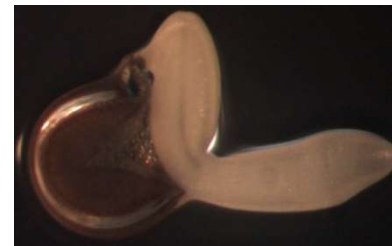
Figure 4.4.3. Effect of heat stress on seed germination of the *eTM-miR165/166* and wild type plants. (a). Rate of germination of the *eTM-miR165/166* and wild type was measured under heat stress. (b) and (c). Growth of *eTM-miR165/166* and *Wt Col* germinated seeds respectively after 3rd day of germination upon heat treatment under stereozoom microscope. (d) and (e). Germination phenotype of *eTM-miR165/166* and wild type seeds upon heat stress after 3 day of germination (DAG3).

(a)



DAG3

(d)



(e)

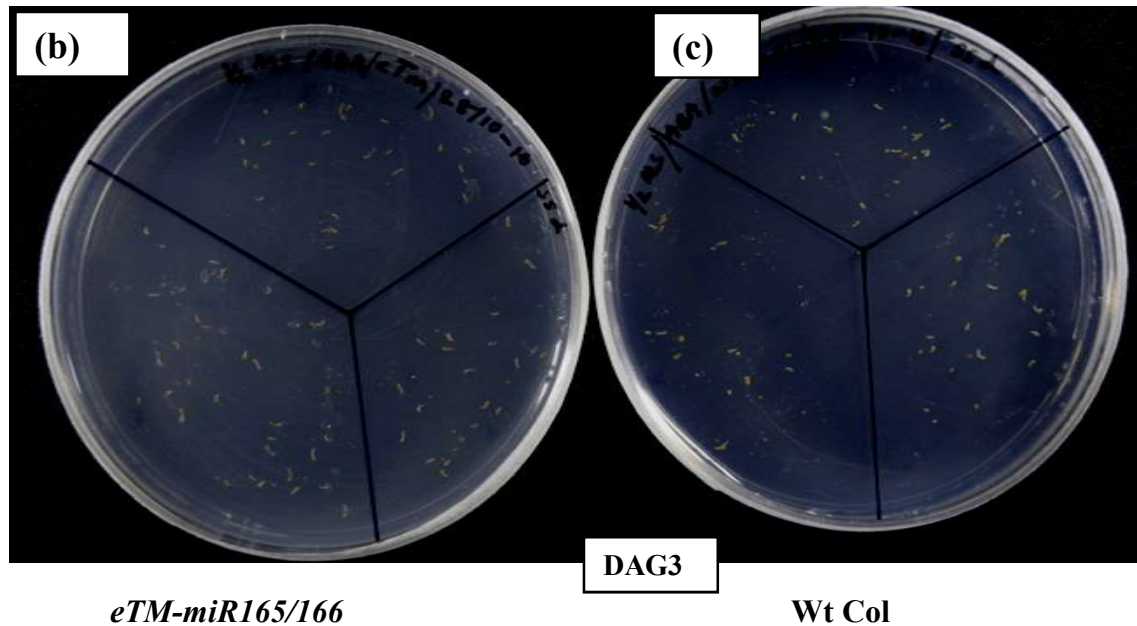
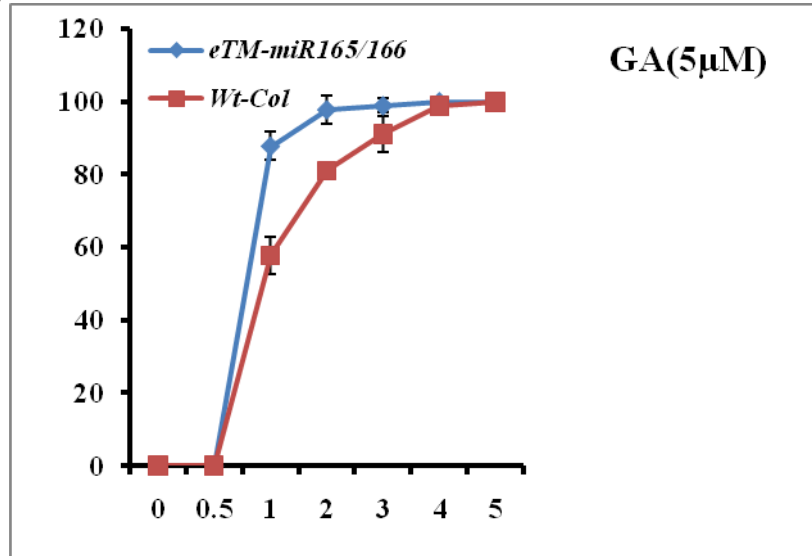


Figure 4.4.4. Effect of ABA(5µM) stress on seed germination of the *eTM-miR165/166* and wild type plants. (a). Rate of germination of the *eTM-miR165/166* and wild type was measured under ABA stress. (b) and (c). Germination phenotype of *eTM-miR165/166* and wild type seeds upon heat stress after 3 day of germination (DAG3). (d) and (e). Growth of *eTM-miR165/166* and *Wt Col* germinated seeds respectively after 3rd day of germination upon heat treatment under stereozoom microscope.

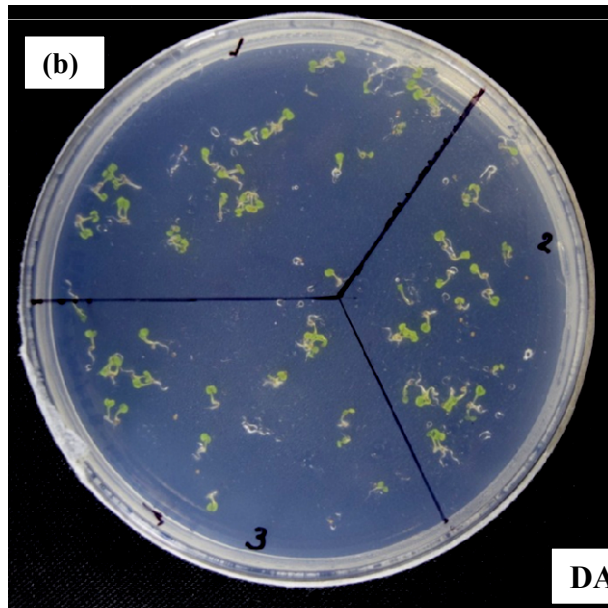
(a)



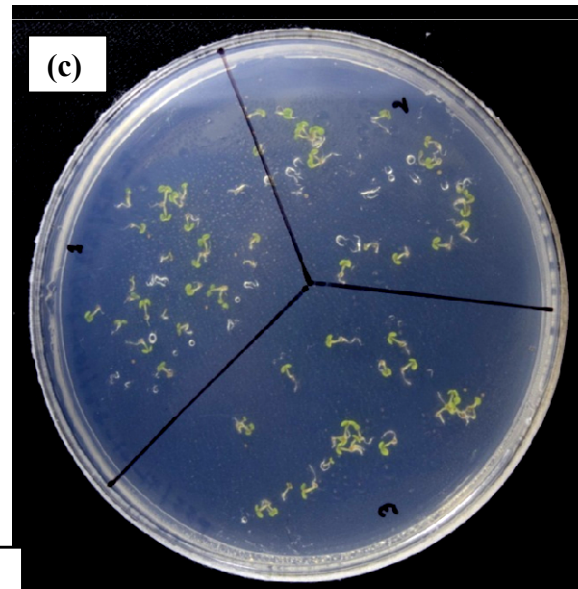
(d)



(e)



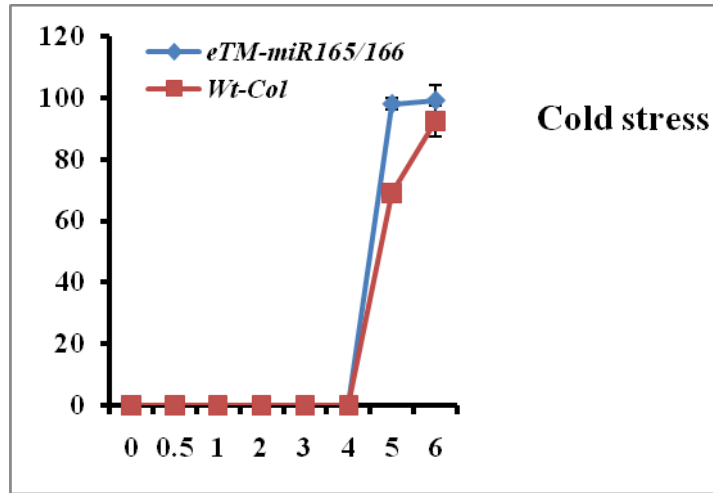
eTM-miR165/166



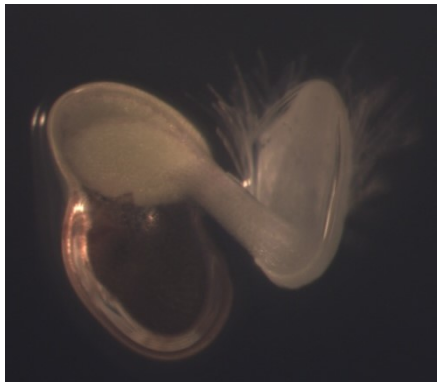
Wt Col

Figure 4.4.5. Effect of GA (5µM) stress on seed germination of the *eTM-miR165/166* and wild type plants. (a). Rate of germination of the *eTM-miR165/166* and wild type was measured under GA stress. (b) and (c). Germination phenotype of *eTM-miR165/166* and wild type seeds upon GA(5µM) treatment after 3 day of germination (DAG3). (d) and (e). Growth of *eTM-miR165/166* and Wt Col germinated seeds respectively after 3rd day of germination upon GA treatment under stereozoom microscope.

(a)



(b)



eTM-miR165/166

(c)



Wt Col

Figure 4.4.6. Effect of cold stress on seed germination of the *eTM-miR165/166* and wild type plants. (a). Rate of germination of the *eTM-miR165/166* and wild type was measured upon cold treatment. (b) and (c). Growth of *eTM-miR165/166* and Wt Col germinated seeds respectively after 5th day of germination upon cold treatment under stereozoom microscope.

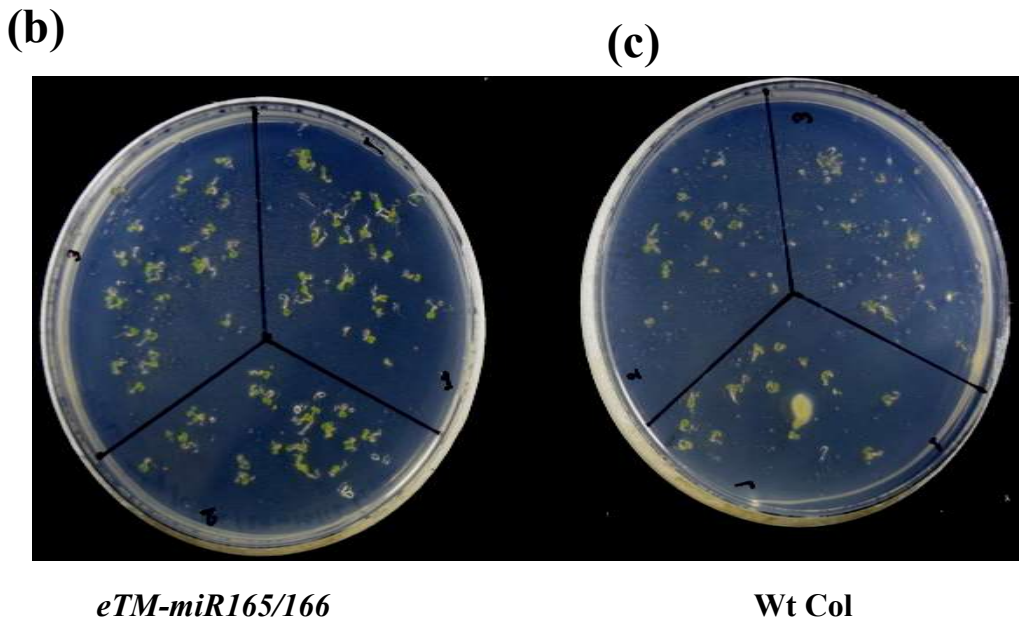
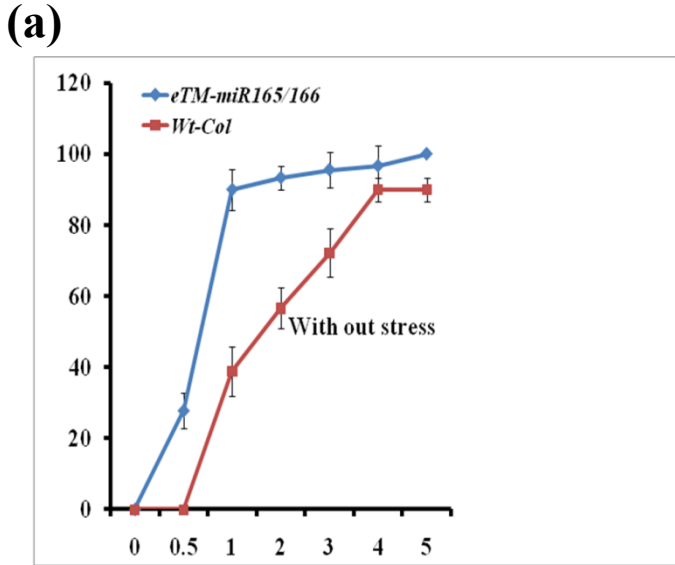


Figure 4.4.7. Seed germination of *eTM-miR165/166* and wild type plants in normal half MS plate (without stress condition). (a). Rate of germination of the *eTM-miR165/166* and wild type was measured under normal growth condition. (b) and (c). Germination phenotype of *eTM-miR165/166* and wild type seeds in normal growth condition after 3 day of germination (DAG3). (d) and (e). Growth of *eTM-miR165/166* and Wt Col germinated seeds respectively after 3rd day of germination in without stress condition (normal growth) under stereozoom microscope.

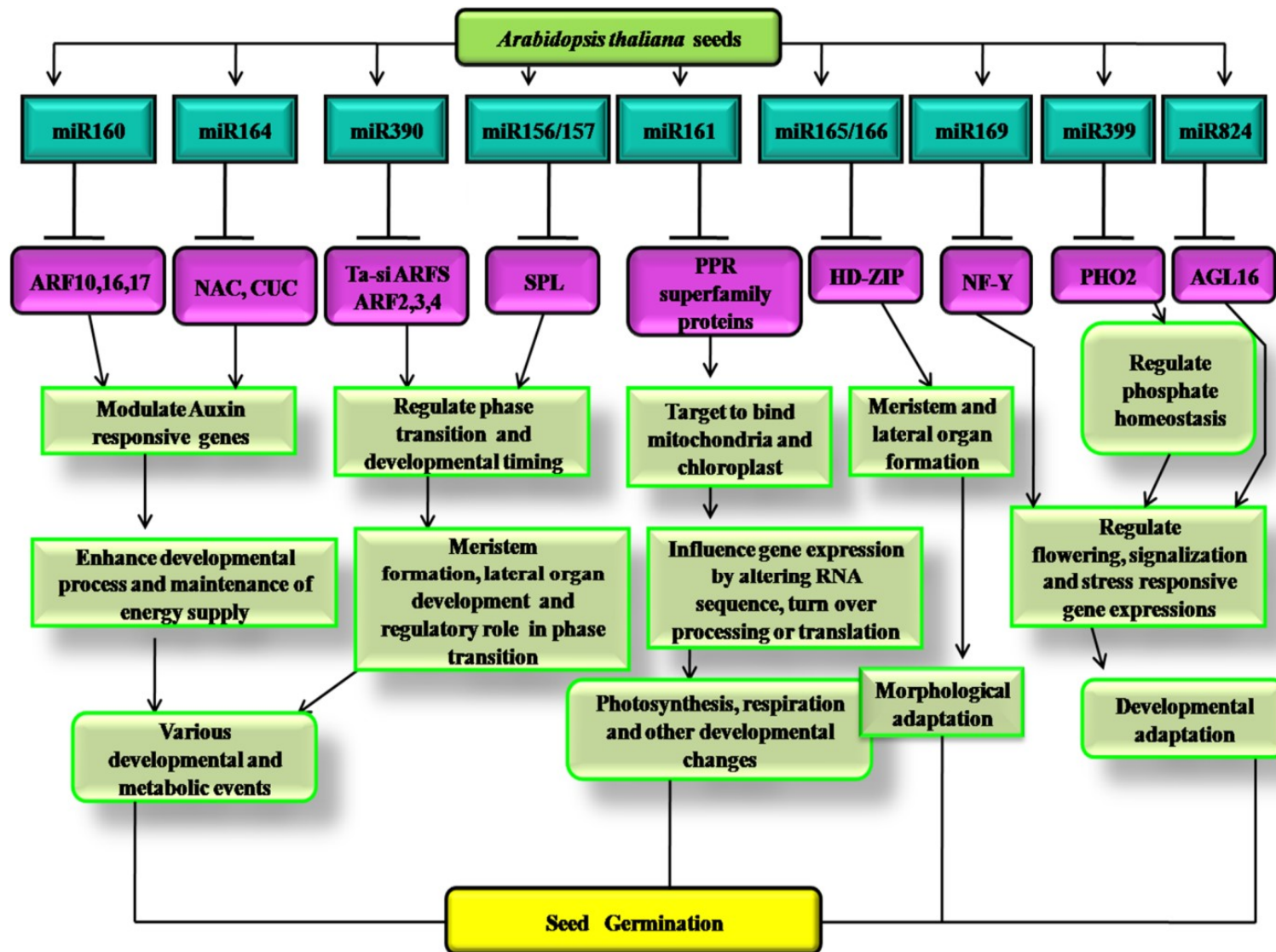


Fig 5.1 The potential regulatory network for miRNAs in seed germination of *Arabidopsis thaliana*.

APPENDIX

Maps of the vectors used in this study

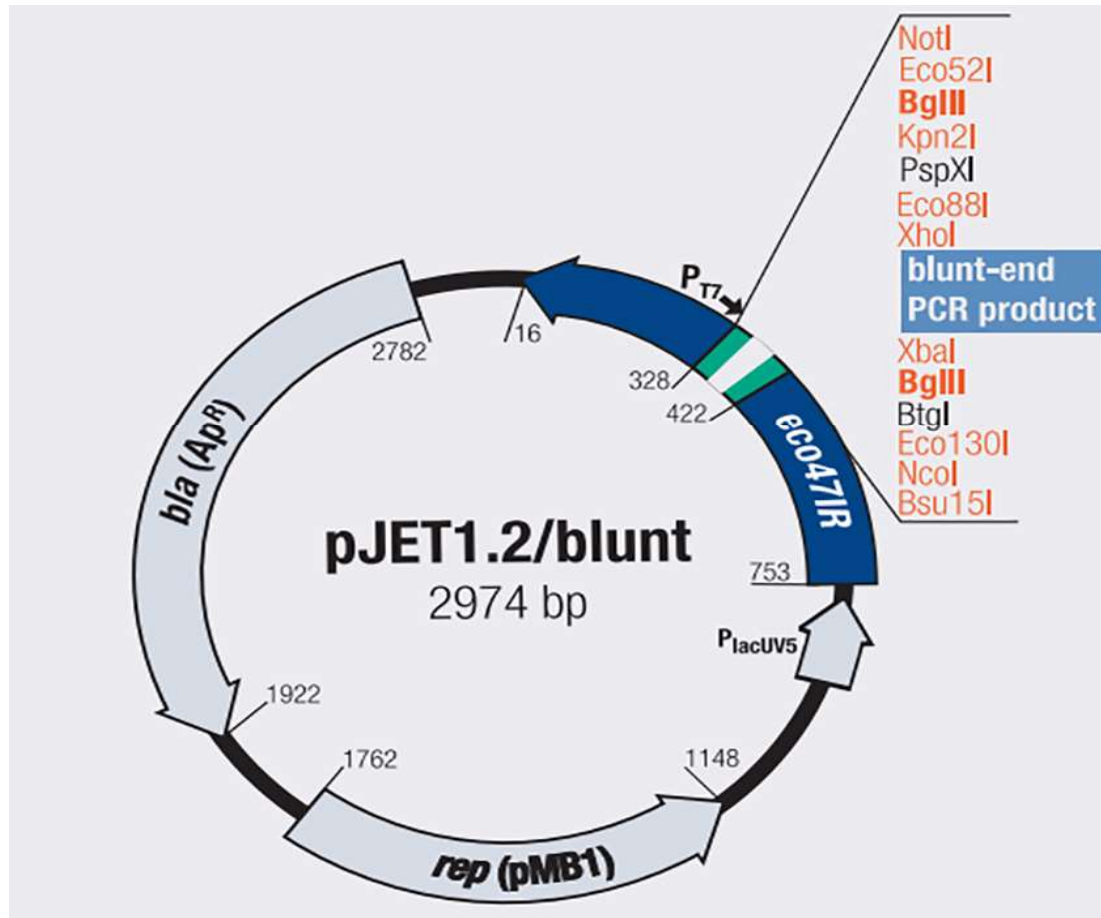


Fig A1. pJET1.2 Vector map

APPENDIX

Maps of the vectors used in this study

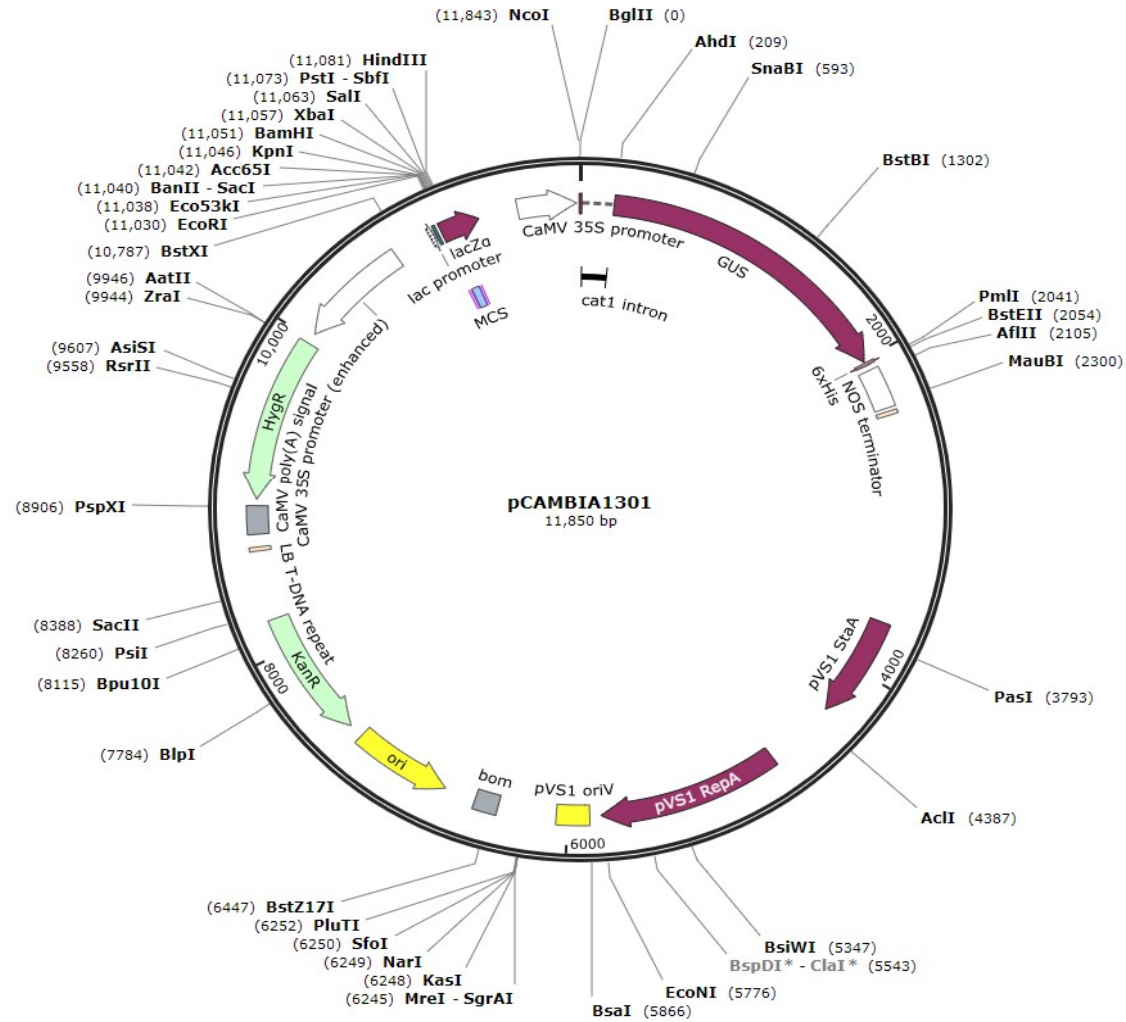


Fig A2. pCambia1301